Abstract

Title of the Thesis: Design and Control of Arm Robot for Rehabilitation of Upper-Extremity Motor Function (REACH)

Ezra Altabet, Honors Thesis, 2019

Thesis Directed by: Dr. Anindo Roy
Department of Neurology
University of Maryland School of Medicine

Stroke is the third leading cause of death in the United States and leading cause of adult disability. As many as 80% of patients with acute stroke and 50% - 95% of chronic stroke patients suffer from upper extremity hemiparesis that impedes mobility and is detrimental to overall quality of life. Repetitive Bilateral Arm Training with Rhythmic Auditory Cueing (BATRAC) is an unpowered end-effector robot designed for rehabilitation of upper extremity motor function in stroke and other neurologic diseases. Despite showing clinical efficacy, the current BATRAC device is therapeutically limited in several fundamental ways, including being unable to collect kinematics, provide visual feedback, or provide motorized assistance to the user during training. In this thesis, a significantly enhanced version of BATRAC, known as the REACH, is developed to address these flaws. This first-generation prototype integrates position sensors, visual feedback, and assistance "as-needed" in addition to enhanced mechanical design. These features are expected to improve neuro-motor and functional outcomes of unilateral and bilateral reach in neurologically disabled populations. The work conducted here also lays the engineering foundation for the development of subsequent REACH versions.

Design and Control of Arm Robot for Rehabilitation of Upper-Extremity Motor Function (REACH)

Ezra Altabet

May 8, 2023

Contents

Acknowledgements

I would like to thank my advisor, Dr. Anindo Roy, for his mentorship, providing me a depth of knowledge in rehabilitation robotics, for his aid throughout the entirety of this project, and for his help in editing this report.

I would also like to take this time to thank others who helped me through this project, including the University of Maryland's Robotics Realization Laboratory (RRL) for providing me both space and resources. I would in particular like to thank RRL's lab manager, Mr. Ivan Penskiy, for always being available when I have been in need of a tool or component within the lab, and teaching me to use a variety of lab equipment.

Lastly, I would also like to thank my friend, John Hamel, who taught me how to utilize the necessary machining for this project as well as for always being a curious mind with which I could bounce ideas off of.

1 CHAPTER 1. INTRODUCTION

1.1 Stroke as Debilitating Disease

Stroke is the third leading cause of death in the United States and leading cause of adult disability. Roughly 800,000 individuals in the US and 17 million worldwide develop or suffer from stroke. Although incidence rates have remained constant over the last 3 decades, mortality and stroke severity have declined. More stroke patients every year, therefore, experience disability and find themselves in need of rehabilitation. Brain lesions due to stroke are highly likely to appear in regions of the brain that affect motor function, leading to hemiparesis and other significant motor deficits that highly impair the stroke victim's quality of life. As many as 80% of patients with acute stroke and 50% - 95% of chronic stroke patients suffer from upper extremity (UE) hemiparesis [1–3]. Most tasks are bilateral in some capacity, making reduced functionality in even one arm debilitating. Upper extremity hemiparesis has been shown to impair the ability to pursue core activities of daily living (ADL) such as dressing, bathing, and toileting, as well as mobility functions, such as carrying objects [4]. Only 5% of adults regain full arm function post-stroke, and 20% regain no functionality whatsoever [1].

1.2 Treatment Paradigms for Stroke

Stroke recovery is often broken down into three phases:

- Early (acute) phase -– ending roughly 2 weeks after stroke
- Subacute (re-organization) phase -– ending roughly 3 months after stroke
- Late (chronic) phase — begins after subacute phase [5]

Standard physical therapy is focused on the subacute phase of stroke, primarily because it is believed that after this period, spontaneous neural recovery ceases and further formal therapy will be of little or no aid [5, 6]. This window of time was determined to be before approximately 8.5 weeks for mildly impaired stroke patients, 13 weeks for moderately impaired and 20 weeks for severely impaired patients post-stroke [6]. Traditional physical therapy methods for stroke rehabilitation have been largely built around passive movements of the arm and compensatory movements of the non-paretic arm [7]. However, recent monkey models have demonstrated that active, or "forced-use" physical therapy paradigms, in which the subjects were forced to actively use their paretic limb, produced functional recovery and cortical reorganization well beyond 3 months post-stroke.

One common rehabilitation paradigm is Constraint Induced Training (CIT), which entails forced-use of the paretic arm by constraining the unaffected arm, and includes the principles of "time-on-task" and behavioral conditioning or shaping. CIT studies in patients with mild chronic UE hemiparesis have demonstrated modest functional gains [7–12]. An alternative unilateral method that also relies on intense repetition is the use of robots to assist with arm movement, for example, the MIT MANUS. In this case, the robot provides resistance to the user when the user is capable of providing force, but provides physical assistance when needed by the patient. A host of studies have shown minor benefits of the device in comparison to traditional physical therapy (TPT) alone, and appears to have greater potential for those more severely impaired [13]. These benefits are a result of 3 underlying therapy principles: repetition of task ("Time on task"), forced-use, and attention to task. These principles appear to be necessary components of

training to have an impact on function as well as facilitate physiological changes in the brain [14].

1.3 The BATRAC

1.3.1 BATRAC Design Consideration

A more effective, and well documented upper extremity rehabilitation technique that utilizes the "forced-use" paradigm is bilateral arm training – training the paretic arm in a synchronous fashion with the nonparetic arm. Repetitive Bilateral Arm Training with Rhythmic Auditory Cueing (BATRAC) is a medical device that takes advantage of the forced-use bilateral movement paradigm by encouraging the patient's use of rhythmic reaching and retrieving actions in either a symmetric (both arms simultaneously reaching/retrieving) or anti-symmetric (one arm reaching while the other retrieves, and then alternating) fashion, using a metronome to cue the patients [14]. A render of the BATRAC is shown in below in figure 1.

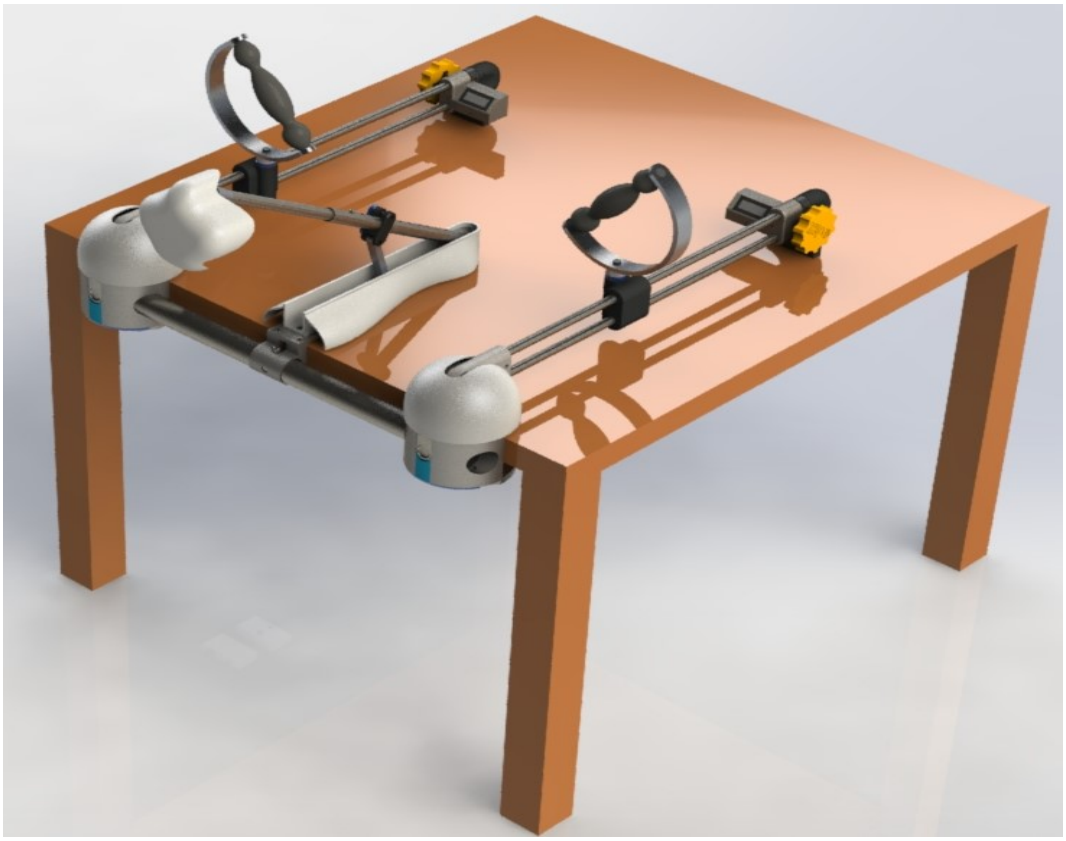

Figure 1: BATRAC mounted on a table: The user sits at the base of the table and pushes the handles with their hands.

BATRAC was engineered on seven motor learning and motor control principles:

1. Task-specificity: This is accomplished through mimicking everyday actions of reaching and retrieving by requiring the user to extend their hand from a close distance to a maximum reach point, then mimicking retrieval through the user's hand returning to home position. Evidence suggests that neuromuscular synergies are organized in a task-specific manner and that motor skill learning is task-specific [15].

2. Repetition and forced-use: Rhythmic repetition and forced-use of an action is well-known for facilitating motor learning and promoting neural plasticity. In a randomized study, functional imaging (fMRI) has shown that new foci or contralesional as well as ipsilesional neural activation for paretic arm movement occurs after BATRAC training, but not after dose-matched therapeutic exercises. [4]. BATRAC forces patients to repeat reaching and retrieving actions through uncoupled handles, ensuring that both arms exert force in order to move.

3. Feedback: Auditory feedback allows the user to hear the delay between their movements and their expected movements set by a metronome.

4. Goal setting: By providing feedback, the user, through focusing on the beat set by a metronome, is able to manually adjust their movements in order to move in accordance with the prescribed beat. In addition, the BATRAC also has a manual stop that adjusts at the beginning of each session to act as an extension goal for that training session. Many studies have demonstrated the importance of goal-setting in increasing motivation and learning [16].

5. Sensory-motor entrainment: Entrainment through auditory cuing ensures the repetition is of the same movement, promoting task-specificity. It should be noted that utilization of entrainment between the motor system and extrinsic auditory sound is a recent development in rehabilitation [16, 17].

6. Bilateral coupling: This synchronization between the paretic and nonparetic arm is theorized to result in a facilitation effect from the nonparetic arm to the paretic arm. In other words, the paretic arm over the course of bilateral movement "relearns" its movement by using the nonparetic arm's movement

as a frame of reference. Several experiments support this claim. Nondisabled persons, for example, when initiating bimanual movements simultaneously, produce arm movements in unison that supersede individual arm action, demonstrating that both arms have the capacity to act as a coordinative unit in the brain [18,19]. Therefore, the neural basis can likely be attributed to interhemispheric disinhibition via the corpus callosum and the use of uncrossed corticospinal pathways.

7. Stable movement patterns: By ensuring the patient reaches and pulls back both arms simultaneously for part of their training, patients benefit from a more stable coordination pattern as evidenced by studies in shoulder flexion/extension, elbow flexion/extension, wrist pronation/supination, and finger abduction/adduction [20–23].

1.3.2 Clinical Findings using BATRAC

A pilot study demonstrated that 6 weeks of BATRAC improved motor function in several key measures of sensorimotor impairments, functional ability (performance time) and functional use in the paretic arm of chronic stroke patients. There improvement were, furthermore, maintained at two months after patients stopped training, suggestive that the motor improvements were potentially durable [4]. Others have also noted the benefits of bilateral training including immediate, clinically and statistically different improvements compared to baseline practice of unilateral, bilateral with the nonparteic arm guiding the paretic, and bilateral with arms doing 2 different tasks [24]. Other studies have shown that a coupled protocol of electromyogram (EMG)-triggered stimulation with bilateral movement was better than EMG-stimulation with unilateral move-

ment, which in turn was better than the control group [25]. 6 weeks of repetitive non-progressive training with the BATRAC was also shown to improve UE motor function in mild and moderately affected patients well beyond the three-month period (i.e. patients with chronic hemiparesis) [14]. A preliminary randomized study showed through functional Magnetic Resonance Imaging (fMRI), that new foci of contralesional as well as ipsilesional neural activation for paretic arm movement occur after BATRAC training but not after dose-matched therapeutic exercises (DMTE) [4].

1.3.3 Advantages of the BATRAC

The BATRAC has been shown to be comparatively effective for the following reasons:

- It is effective for moderately and mildly affected patients in contrast to CIT.
- It is less time-consuming than either CIT or other typical robot paradigms.
- It is less expensive than compared to current robot therapies on the market.

Further, the BATRAC demonstrates advantages over other bilateral training methods for the following reasons:

- It is easier to administer, cheaper, and focuses on the whole arm compared to EMG-triggered stimulation.
- It has more repetition and can more positively affect more severely impaired patients than CIT.

1.3.4 Drawbacks of the BATRAC

The current BATRAC, however, is quite limited for a number of reasons. First, the device as-is is not instrumented for acquisition of arm displacement data. This means that more traditional and qualitative scales of rehabilitation, such as the Wolf and Fugle-Meyer, must be utilized rather than modern quantitative scales, such as jerk measurement, peak velocity, tent matrices, and MAPR. This lack of information reduces our ability to accurately assess the patient's progress over the course of therapy.

Second, whereas auditory cuing has been effective, the device would be enhanced further through visual cuing in the form of a task-specific video game. On-screen visual representation allows for real-time visualization of excursions made by the patient when using the device, but more importantly, allows for a more finetuned goal setting in which the patient can achieve real-time goals to reach a quantifiable distance. Visualization thus is clearly shown to provide far more information and therefore motivation, to the patient during therapy.

Thirdly, the lack of actuators and sensors prohibits the potential of the device to exploit impedance control, a method of coaxing motor learning in which, over the course of movement, machine learning algorithms are used in combination with actuators to modulate end-effector mechanical impedance rather than position or force, and guide the user into a rhythmic pattern of bilateral extension and retrieval by calibrating the assistance/resistance supplied by the actuator to the movements of the user. This control algorithm in combination with highly backdrivable actuators (gearless, linear screw drives rendering negligible stiction) translates to the user's perceived "robot feel" and has been shown to be

a very effective rehabilitation method in comparison to physical therapy without impedance control [26].

1.4 Goal of this Project — REACH Phase 1

Drawing on the operational and therapeutic limitations of the BATRAC as outlined above, a new version of the BATRAC, known as REACH, is being developed to address the BATRAC's drawbacks above. The purpose of this project was to create a first prototype of the REACH using Minimum Viable Product (MVP) criteria, as will be further discussed in later sections. The REACH Phase 1 was driven by two primary technological challenges:

- *Therapeutic Efficacy* – development of an ergonomic and actuated device that patients can safely use for linger time periods while receiving as-needed assistance. Ergonomics further includes stable and comfortable human-device fit, while actuation entails choice of optimal hardware and control strategy for enhanced patient outcomes.

- *Clinical Usability* - to develop an instrumented device interfaced with a videogame. Instrumentation entails appropriate choice of sensor to calculate key movement metrics to index patient recovery. Videogame development entails a simple yet engaging visual task that is customizable (both manually and through machine learning) to patient deficits and recovery to enhance motivation though goal-setting and performance feedback.

1.5 Outline of REACH Phase 1 Development

The course of REACH Phase 1 has been broken down into 5 major tasks, 3 of which have been the focus of this project.

Task 1: Ergonomic and Modular Design: Handle Ergonomics: The patient interfaces with the rehabilitation device via the handles. Usage of these handles requires constant forearm rotation or pronation, increasing strain which restricts the patient from following the natural arm movements necessary for training. The handles themselves also require the user to utilize particularly awkward finger positions. A redesign of the handle is thus needed such that the user will be able to retain a neutral position throughout their use of the device. Elevation Backlash: The system is intended to be used in both horizontal and inclined positions to allow for training different arm motions. The current BATRAC's security allows the system to shake intensely as the patient pushes the handles along the rails of the device, thus hindering any rehabilitative effects of the device. The device must thus be redesigned to prevent any shaking of the device during operation. Elevation Change: In order to allow the device to achieve multiple angles of elevation, the current method requires the rails of the BATRAC to be pushed into the shoulder of the device, which disengages a locking mechanism, allowing the user to change the elevation angle of the device. This method, however, invokes loose fitting attachments that contribute to the device's shakiness. A redesign is thus needed to increase stability for different elevations. Weight Reduction: The device as-is is bulky, and difficult to dis/re-assemble, making the device awkward to transport between locations. A redesign taking into consideration weight and Design for Assembly considerations is needed.

Task 2: Real-Time Electronic Feedback: Use of the BATRAC typically produces gains in Range of Motion (RoM) on the scale of centimeters. These gains are often too small for a patient to perceive. Electronic instrumentation is thus needed to more finely track the movements and gains of the patient in order to increase motivation to continue therapy, as well as act as biofeedback for the patient over the duration of a treatment session. This added instrumentation will also enable the patient or therapist to easily set the machine to settings corresponding to outcomes of the previous treatment session, allow for the potential of visual feedback (Task 4: Visual Interaction), and enable Task 3: Design and Control.

Task 3: Design and Control: Hardware: The components enabling actuation must saitisfy constraints including low friction, back-drivability, inertia at the robot end-effector, with an upper bound in overall robot weight for sufficient range of forces, stiffnesses, and impedances at the end-effector. Therefore, it is crucial to select the appropriate motor, which will be determined through values of peak torque and back-drivability requirements. As a result of previously acquired arm movement data from healthy subjects, a low intrinsic end-point impedance is required, low inertia (0.6-1.5 kg), friction (0.5-1.1 N), and capacity to produce between 0 and 45 Newtons of force.

Task 4: Visual Interaction: Provision of a method of visual feedback has been theorized to tremendously increase efficacy in patient rehabilitation. This is to be accomplished via an on-screen training application to be implemented and tested. The function of this app is to not only make patients aware of their real-time movements but also assist in enhancing attention and motivation throughout their treatment session. This will be accomplished via two separate training mod-

ules: one focused on improving paretic range of motion (RoM), the other improving inter-limb symmetry.

Task 5: Clinical Prototyping: Iterations of tasks 1-4 will over time will produce a design that can be drafted for clinical pilot testing. At this stage, considerations will be made for design freeze for submission to the FDA as a medical device. Based on advice from Patsy Trisler, an FDA consultant, a plan will be put forth to go through an FDA Expedited Approval Process (EAP) for devices that address an unmet need for life threatening or irreversibly debilitating diseases or conditions.

The above modifications have been summarized in the table below:

FEATURE	BATRAC	REACH
Instrumentation	✗	✓ Position Sensor(s)
Control	✗	✓Impedance (Moving Box) Control
Functional "Assist" Modes	✗	✓Active Assist (As-Needed),Resist
Stimulation	✗	✓ Visual (± Auditory)
Therapy Progression	✗	✓ Machine Learning

1.5.1 Scope of this Project

The above outline models the stages of the entire development of the REACH Phase 1. This project, however, will be focused primarily on key first prototyping stages of Real-Time Electronic Feedback, Actuation and Control, and Visual Interaction (Tasks 2-4), following Minimum Viable Product (MVP) guidelines, which will be introduced at the beginning of each of the following chapters.

1.5.2 Prototype Reference

The following chapters will go into detail regarding the additions and modifications made to the BATRAC in order to develop the REACH Phase 1 prototype. The following rendered image of the full prototype for right arm hemiparesis with additions and modifications has been provided in order to provide the reader a frame of reference for the following chapters' discussions, analyses, and exploded views.

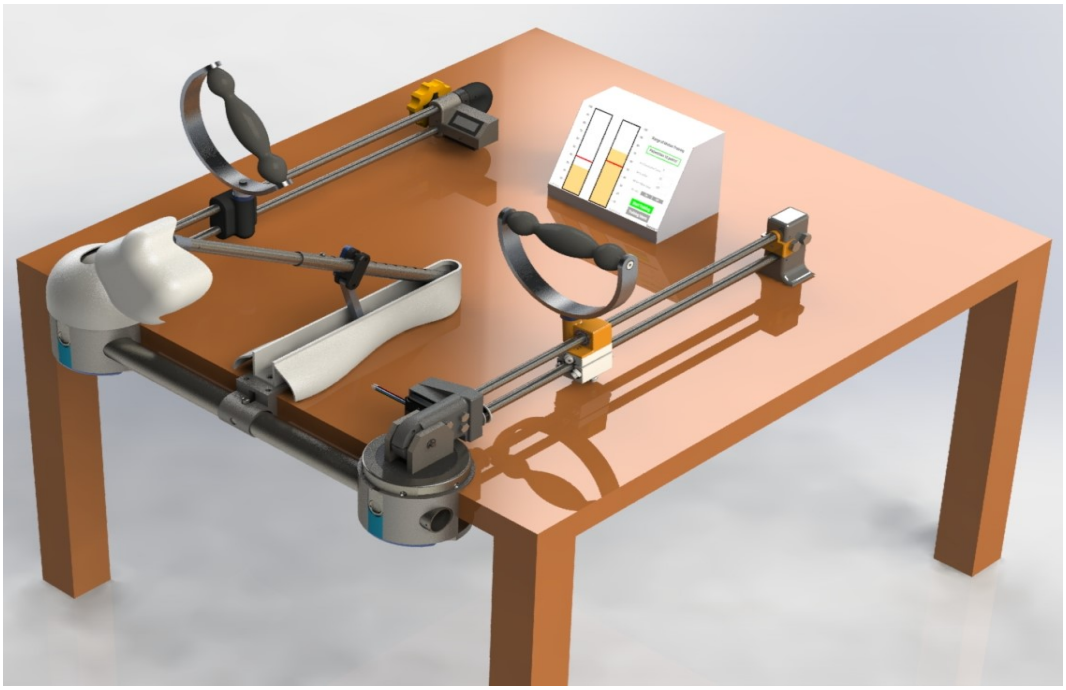

Figure 2: Current REACH prototype for right arm hemiparesis

2 CHAPTER 2. SENSORS AND BIO-FEEDBACK

2.1 Purpose of Sensory/Bio-Feedback

2.1.1 Rationale for Instrumentation

Gains made during BATRAC training are typically on the magnitude of centimeters, which is much too small for a patient to perceive on their own. In order to compensate for this, a kinematic sensor collecting data of patients' movements over the course of training, patients and clinicians will more easily be able to detect these incremental changes. Augmentations in this way may lead to increased work effort, increased attention to task, and potentially improved patient outcomes.

Further, without kinematic data, physical therapists and clinicians must rely on more traditional and qualitative scales of rehabilitation, such as the Wolf and Fugle-Meyer. Both of these assessments do not utilize quantifiable data, and simply use an implicit scale of the patient's degree of success for a range of functional tasks. This of course allows for inherent biases on the part of the exam administrator. More modern assessments have begun to utilize quantifiable clinical rehabilitation metrics such as jerk measurement, peak velocity, tent matrices, and MAPR. These metrics, given their dynamic nature, are only capable of being acquired through sensors that automatically record and process user movement, and would be much too cumbersome to be acquired by a practitioner taking a series of measurements. This data can be collected automatically via displacement sensors, which in turn can be quickly processed into more meaningful data. The addition of a kinematic sensor also allows for more complex feedback control such as Visual Feedback, (as will be further elucidated in the next section), as well as closed-loop actuated assistance/resistance.

2.1.2 Rationale for Visual Feedback

It is true that auditory cuing has been shown to be effective in providing motivation and bilteral coordination during physical therapy. However, theory suggests the device would be enhanced further through visual cuing in the form of a task-specific video game. On-screen visual representation allows for real-time visualization of excursions made by the patient when using the device, but more importantly, allows for a more finetuned goal setting in which the patient can achieve real-time goals to reach a quantifiable distance. Visualization, although not formally studied, offers great potential to provide far more information and therefore motivation, to the patient during therapy.

In order to maximize user patient motivation, this videogame will become part of a fully customizable training app with which the patient can see their rehabilitation status over time, as well as build personalized training module sequences, the details of which will be further elaborated in the coming sections.

2.2 Go/No-Go Criteria

The section's exact specifications were conceived from go/no-go criteria in the implementation of kinematic sensors necessary for data collection and development of an on-screen visual training tool to be used both for visual cueing as well as for goal setting; two of three items mentioned above.

Position Sensors: Go/no-go criteria for the kinematic sensors were decided by successful integration and confirmation of successful precision. Successful integration of the sensors was designed by three benchmarks: providing readouts, successful mechanical embedding of the sensors into the BATRAC, and successfully providing numeric readouts. The go/no-go criteria for successful precision

was given to be met if the sensor outputs produced output readings with a standard error (SE) below five millimeters. Sensors were determined through a series of design and performance constraints including accuracy/resolution/SNR, field of view, drift, sensitivity to ambient light, and cost.

Training App: Go/no-go criteria for the training app were decided by integration of screen design and visual objects, visual representation of real-world arm movements onto screen movements, machine learning to adjust task difficulty to real-time performance, and real-time computation and display of one or more performance metrics (e.g. maximum extension, minimum jerk).

2.3 Integration of Sensory Feedback

2.3.1 Choice of Position Sensors

Several sensors were initially considered for use as this kinematic sensor, including accelerometers, magnetic encoders, time-of-flight sensors, and linear encoders (mechanical). The sensor was chosen through a series of design and performance constraints including accuracy/resolution/SNR, drift, sensitivity to ambient light, and cost. A table of the analysis is presented below. Each feature was given an associated "High" and "Low" qualifier respectively, to identify if the system is optimized by maximization or minimization of the corresponding feature. Each sensor was then given a qualitative score of "good", "fair", or "poor", denoting how the sensor's effect on the given parameter benefited or hurt the project:

FEATURE	**REQUIR-EMENT**	**Linear Encoder**	**Magnetic Encoder**	**Accel-erometer**	**Time-of-Flight**
Friction	Low	Fair	Good	Good	Good
Accuracy	High	Good	Good	Fair	Fair
Drift	Low	Good	Good	Poor	Good
Light Sensitivity	Low	Good	Good	Good	Fair
Ease of Integration	High	Poor	Poor	Fair	Good
Cost	Low	Poor	Poor	Fair	Good

Linear encoders, a mechanical sensor, were excluded because they were the most likely to cause unwanted friction for the user. Accelerometers, measuring displacement indirectly through acceleration, were excluded because of their potential to produce false values as a result of drift over time. The time-of-flight sensor, a rather inexpensive sensor in comparison to magnetic encoders, was chosen over a magnetic encoder as a base sensor for analysis in order to potentially limit costs to the physical therapist as well as to allow for a simple and elegant robot architecture.

The specific time-of-flight sensor chosen was the VL53L1X Time of Flight Sensor by Pololu. The sensor is a 13mm x 18 mm x 2mm board, with an operating voltage between 2.6 and 5.5 v, and a supply current of roughly 15 mA. The board has a range of 4cm to 400 cm with a resolution of 1 mm. The board has three built-in distance configurations to accurately represent the distance for a given distance range. The *short* range measures up to 130 cm, and has a sampling rate of 50 Hz. The *medium* range measures up 300 cm with a 30 Hz sample rate. Lastly, the *long* range measures up to 400 cm with a 30 Hz sample rate. For all ranges, the best data collection is acquired through minimization of ambient light.

2.3.2 Implementation of Position Sensors

The sensor was integrated into the REACH by creating a tight-fit plastic housing/mount out of PLA. In order to minimize redesigning of the REACH, in the current prototype the sensor was fastened into a housing, which in turn was fastened to the end-cap of the REACH via a bolt. An exploded view is presented below in figure 3. As is evident there is no mechanism for minimizing shock on the sensor. This is because there is no need to mitigate any potential improper readings resulting from the user colliding the BATRAC handle with the sensor housing because the sensor has been shown to not be able to take accurate data in such short range in any case, as will be shown in the next section.

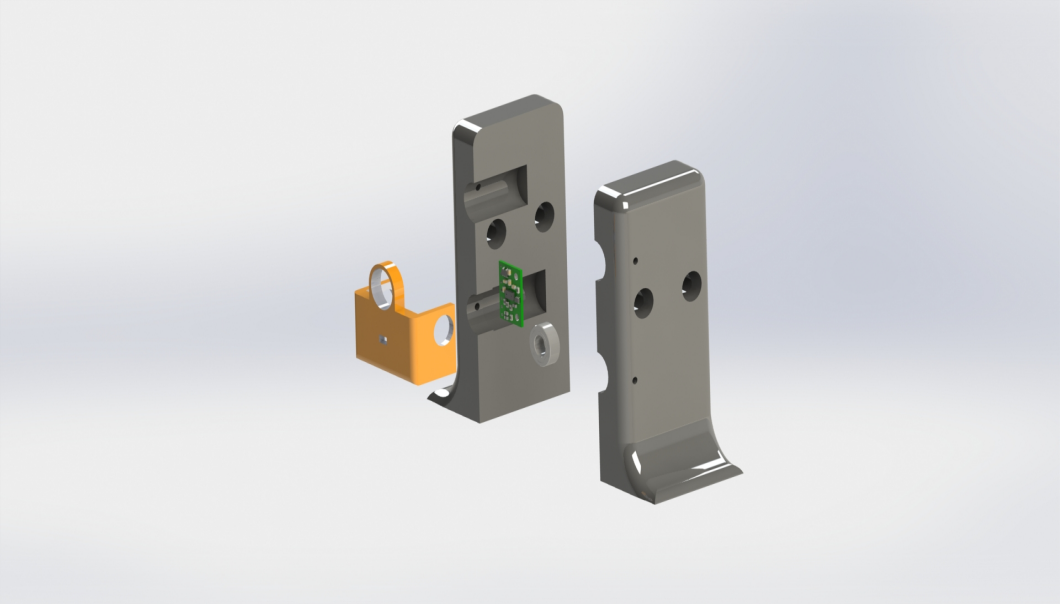

Figure 3: Exploded view of time-of-flight sensor, housing, and mount

2.3.3 Quantification of Sensor Performance

In order to assess the caliber of the sensors, sensor output values were compared against known distances on the BATRAC from 0 to 430 mm. 5 seconds (roughly 45 data points) of distance values were collected for every 10 mm increment. Several metrics were then used to assess the caliber of the sensors. Percent error of the mean recorded values against the external measurement was used to map overall error in measurement by the sensors. The standard deviation was then taken in order to predict the likelihood that the distance data recorded over time by the sensors could be used to create a velocity profile. Lastly, to assess overall repeatability of measurements, the student standard error (SE) was found, and was used to create a 95% confidence interval of sensor values across the distance of the BATRAC arm.

The resulting mean percent error across distance is shown to the right. As can be seen, no reading was detected by the sensor until roughly 40 millimeters, at which its accuracy increased until roughly 370 mm, at which point, the left sensor appears to have stabilized in accuracy, the right sensor then beginning to estimate values greater than recorded true distances. In order to avoid disturbance of the sensor by nearby objects, the field of view of the sensor was minimized.

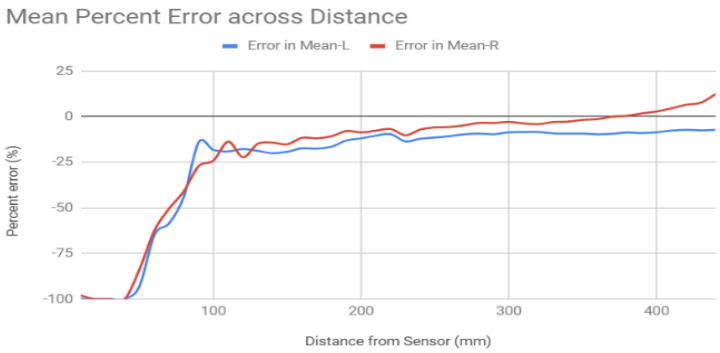

Figure 4: Percent Error

This minimization, however, is most likely the reason for such great abnormalities in error in the short-range region (below roughly 100 mm) detected by the sensors. From the data it can also be seen that there is an initially large percent error and standard deviation, and over increased distance, these metrics become smaller, and therefore, more accurate. However, even with these high standard deviations, a 95% confidence interval shows a measured value will most likely be within 1.4 mm of the sensor's mean measured values for any given distance. This shows that even with a high percent error, its high reproducibility allows for accurate mapping between measured and real values over the course of prototyping.

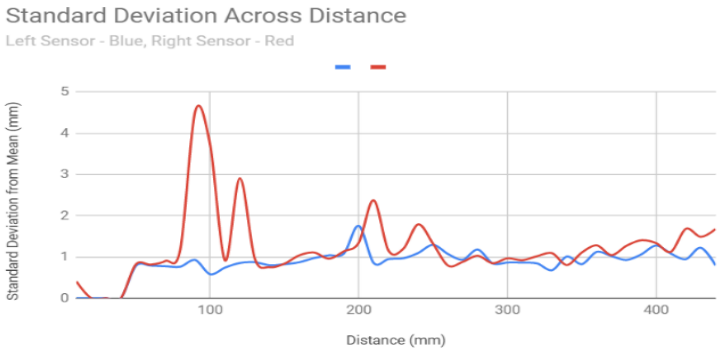

Figure 5: Standard Deviation

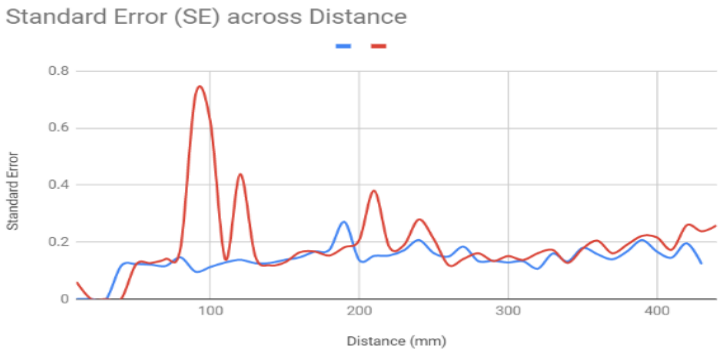

Figure 6: Standard Error

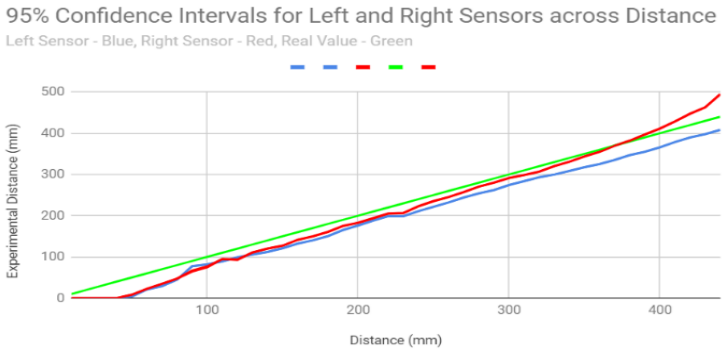

Figure 7: Confidence Interval

2.4 Integration of App

2.4.1 Base Setup and Brief Tour

Hardware: The training app is designed to effectively collect quantitative user data as well as promote visual feedback. This visual feedback is delivered via a touch-screen, connected to a Raspberry Pi (RPi) computer. Distance data and time-stamps are provided to the RPi from an Arduino Feather M0 via a serial connection.

Software: The backend data collection from the Feather, as well the mechanics that drive the app is then processed by a Python script on the RPi. In the current version of the app, the user information is stored locally on the RPi in form of Directories and CSV files, as these files are easily readable by Python and require minimal read/write time. Frontend visuals, however, are provided to the user via the Python module Kivy, an open source Python library specifically used for developing mobile apps and multitouch application software.

Login Page: On executing the app, the user is required to enter a 7-digit login code. This code is associated with a preexisting profile of the user, and further

contains any data that has been collected during the patient's use of the device. If the user enters a 7-digit login that is not found in the RPi's local database, the user will have the option to create a new account. If they choose this option, they will be prompted for several key pieces of information needed by the app in order to tailor the app to the new user. This includes selectng the arm that requires rehabilitation as well as the length of their arm. This information will then be used to normalize the app parameters to the specifics of the patient, as will be seen in the following section.

Training Modules: This is the bulk of the app. In this page, the user can decide to choose Range of Motion (RoM) or Symmetry therapy modules. In RoM, the user trains with the goal of improving their maximum extension (outward reach) and flexion (inward reach). In Symmetry, the user trains with the goal of maintaining continuous symmetry of their hemiparetic and healthy arms. This module has two formats: Symmetry, which requires the user to minimize the distance between their two hands, and Anti-Symmetry, which requires the user to maintain symmetry between their two hands about a point located on the device one half arm's length away from the user. The user can choose to quit these modules at any time.

Program Selection: The user also has the option to, rather than choose each training module individual, create an individualized training program, where the user can select any order of any number of the 3 training modules (RoM, Symmetry, Anti-Symmetry), as well as the number of minutes they want each training module to be active before switching to the next one as shown in figure 8.

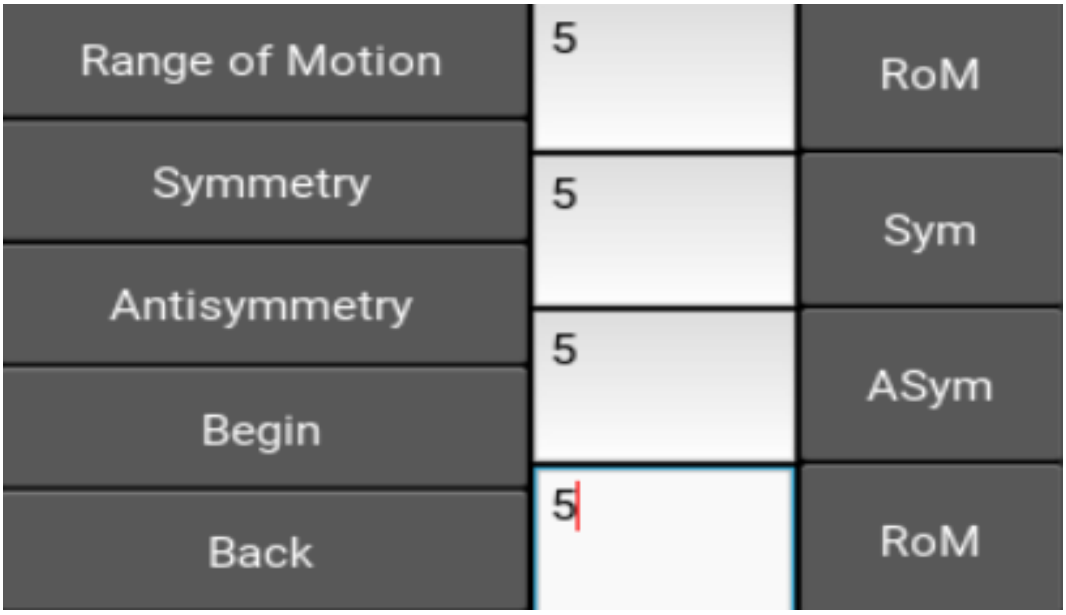

Figure 8: Program Selection: The user selects a custom sequence of training programs

Each time the user creates a new training program, this is stored in a "Recent Programs" page that can be accessed at any time, even after closing and-reopening the program, as shown in figure 9.

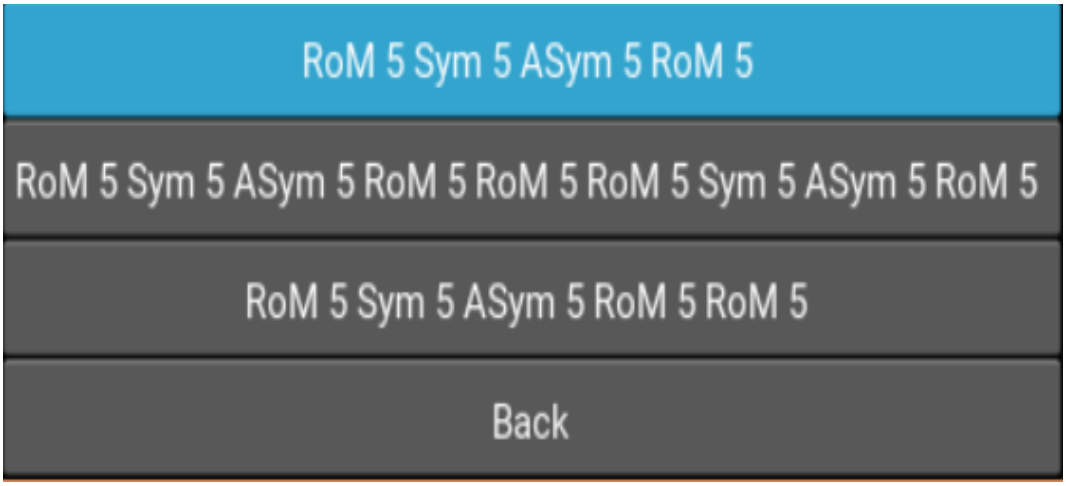

Figure 9: Recent Programs: The user can return to previous programs

This was designed with a two-fold intention: the first was to create a system in which a user can maximize their training while minimizing their time needlessly pressing buttons; the second was to provide flexibility for PTs by allowing them to pre-select training programs to be used by their patients.

2.4.2 Range of Motion versus Symmetry Modules

In order to provide a method of visual feedback for the patient, an on-screen training app was implemented. The use of a training app not only allows the user to physically see the real-time results of their movements, but also allows for complex goal setting that cannot be provided through audio cuing alone. This not only operates as a biofeedback for patients to make self-corrections of their movements, but also assists in retaining the attention and motivation of patients throughout their treatment session. These tasks were accomplished through two separate in-app training modules, one designed to reinforce the goal of RoM of the paretic arm in figure 10, the other dedicated to improving interlimb symmetry in figure 11.

The goal of the RoM module is simply to, over time, increase the user's paretic arm's range of motion. More formally:

$$RoM = x_{max} - x_{min} \tag{1}$$

where x_{max} and x_{min} are the maximum and minimum distances the user is able to traverse over the course of a single excursions.

The symmetry and anti-symmetry modules utilize the symmetry metric of

$$SI = N - \sum_{i=1}^{N} |1 - \frac{x_{P,i}}{x_{NP,i}}| \tag{2.1}$$

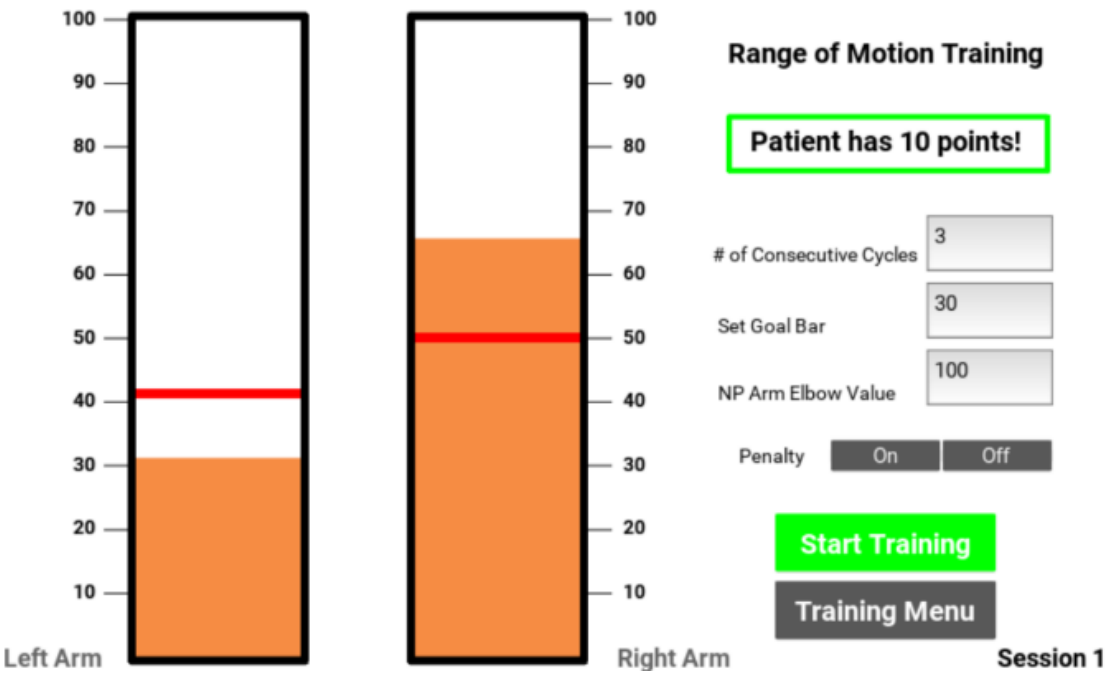

Figure 10: Range of Motion Module

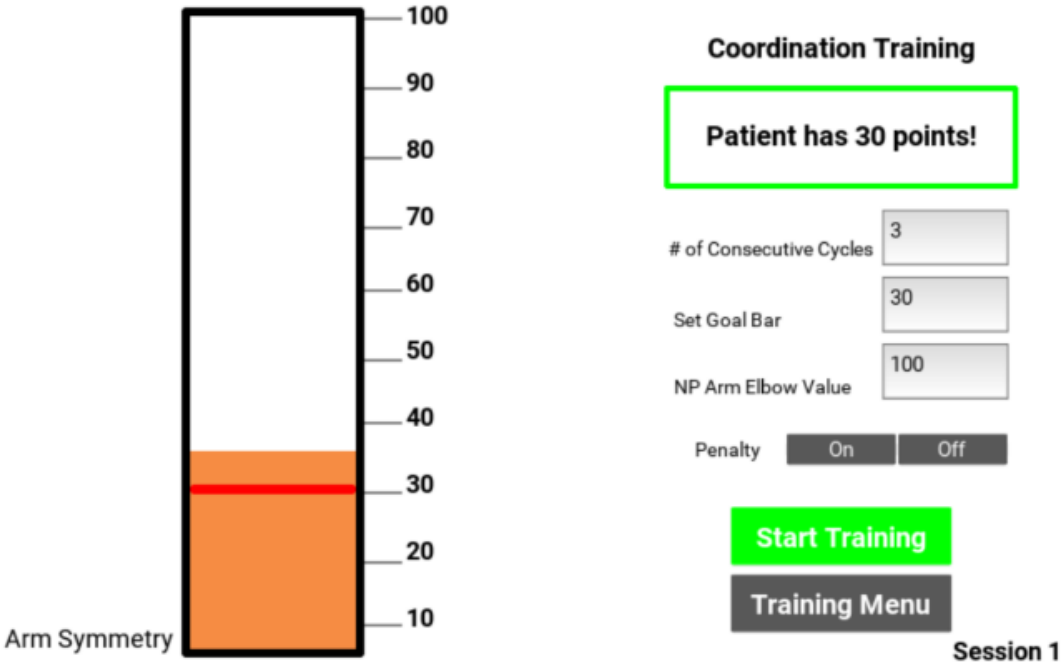

Figure 11: Symmetry Module

where $x_{P,i}$ and $x_{NP,i}$ are the displacements of the paretic and non-paretic arms at a given sampling instant, i, N being the total number of samples collected for a given excursion. $SI = N$ and $SI = 0$ correspond to perfect perfect symmetry and perfect asymmetry respectively.

The range of motion module simulates the above RoM metric, figure 10 displaying two separate orange bars, one for each arm, that change height depending on the distance, x_i the user has moved on the BATRAC in a given sampling instant. The bar representing the paretic arm is normalized to the non-paretic arm, such that the bar reaches 100% of its possible height when the user's paretic arm extends to the maximum extension of the non-paretic arm. The symmetry module in figure 11, rather than displaying one bar for each arm, displays a single bar, which increases in height on the screen with improved inter-limb symmetry, where 100% of its height is attained when there is complete symmetry between the patient's two arms.

It has been hypothesized that users respond better to bars increasing rather than decreasing. Therefore, whereas, the REACH symmetry module utilizes equation 2.1 directly, the REACH's antisymmetry module implements a modified asymmetry equation of:

$$ASI = \sum_{i=1}^{N} |1 - \frac{x_{P,i}}{x_{NP,i}}| \tag{2.2}$$

in order to allow greater antisymmetry to be reflected as a greater ASI value.

Both of these modules have incorporated machine learning as well, through implementation of real-time goal setting through a red bar that ascends or descends on the screen depending on the performance of the patient. For every ten cycles of movement by the patient, if at least 60% of excursions have resulted in a maximum extension above the red line, the line will move up by 20% of its current

value. (A points counter at this time will add ten points to the user's overall score as an added way of representing the user's performance as well as to increase motivation, by establishing the goal of maximizing points and, therefore successful reaches.) Conversely, five or fewer successful movements past the red line will result in the red line descending by 20% of its current value. This allows the user to have consistently and automatically updated goals throughout a single treatment session based on their current capabilities rather than requiring the physical therapist to manually adjust a physical stop. Further, both of these modules offer flexibility to the physical therapist by allowing for a manual override of default parameters, namely the number of consecutive arm movements to be completed per 10 cycles, the initial value of the red bar, and the raw distance/symmetry that 100% represents on the screen.

For reference, the following equations illustrate the logic of the machine learning interface. In the following equations, h is simply an iterator that increases by 1 after the user completes an excursion. Note: in the following piecewise functions, for all cases not specified, the output value of the function is equal to the output value of the function's previous iteration.

n_{e_h} is the number of excursions attempted by the user. If n_{e_h} reaches n_t, the number of attempts at which point the bar height will change, then n_{e_h} returns to 1.

$$n_{e_h} = \begin{cases} n_{e_{h-1}} + 1 & \text{if } n_{e_{h-1}} < n_t \\ 1 & \text{if } n_{e_{h-1}} = n_t \end{cases} \tag{3}$$

For every excursion made prior to n_t, the number of successes n_{s_h} is tallied. An excursion is considered to be successful if the current metric M_{u_h}, reaches a value higher than the current bar height, H. This tally resets after n_t excursions.

M_{u_h} is equivalent to the equations of RoM, SI, and ASI outlined above depending on the chosen training module.

$$n_{s_h} = \begin{cases} n_{s_{h-1}} + 1 & \text{if } M_{u_h} < H_{h-1} \wedge n_{e_h} \leq n_t \\ 1 & \text{if } M_{u_h} \geq H_{h-1} \wedge n_{e_h} = 1 \\ 0 & M_{u_h} < H_{h-1} \wedge n_{e_h} = 1 \end{cases} \tag{4}$$

A unit sign is then determined based on the relative number of successes to the required minimum number of successes, K.

$$n_h = \begin{cases} -1 & \text{if } n_{s_h} < K_{h-1} \\ 1 & \text{if } n_{s_h} \geq K_{h-1} \end{cases} \tag{5}$$

Under normal conditions the goal bar will be raised or lowered by a percentage α of the current bar height H depending if the patient can provide $n_s \geq K$ within n_t excursions where K is equal to the default K value of $K_{baseline}$. However, as the user progresses in their rehabilitation, the patient will reach a point where there is little room left for improvement. Thus, if the patient reaches some coefficient β relative to a final rehabilitation metric L_{arm}, when n_t number of attempts is reached, keep H stationary and increase the minimum required number of excursions by 1.

$$H_h = \begin{cases} H_{h-1} + n_h \alpha H_{h-1} & \text{if } n_{e_h} = n_t \wedge (H_{h-1} < \beta L_{arm} \vee K_{h-1} = K_{baseline}) \\ H_{h-1} & \text{if } n_{e_h} = n_t \wedge (H_{h-1} \geq \beta L_{arm} \wedge K_{h-1} > K_{baseline}) \end{cases} \tag{6}$$

$$K_h = \begin{cases} K_{h-1} - 1 & \text{if } K_{h-1} > K_{baseline} \wedge n_{e_h} = n_t \wedge n_{s_h} < K_{h-1} \\ K_{h-1} + 1 & \text{if } K_{h-1} \geq K_{baseline} \wedge n_{e_h} = n_t \wedge n_{s_h} \geq K_{h-1} \\ K_{h-1} & \text{if } K_h = n_t \wedge n_{e_h} = n_t \wedge n_{s_h} \geq K_{h-1} \end{cases} \tag{7}$$

Both modules, in addition, also will, after fifty cycles, update the user of their overall performance by displaying for thirty seconds, a screen presenting relevant clinical metrics to the user, including mean maximum distance achieved per arm, mean maximum velocity, mean maximum acceleration, and mean maximum jerk. An example is shown below in figure 12.

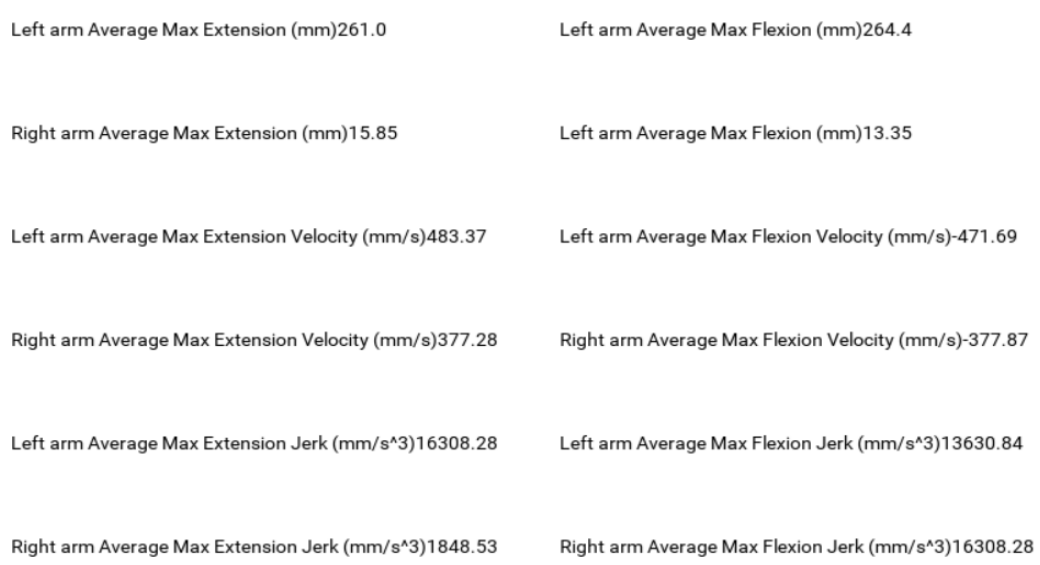

Figure 12: User metric outputted every 50 excursions

3 CHAPTER 3. DESIGN AND CONTROL

3.1 Purpose of Design and Control

In the brain, some key functions of the pathways within the motor cortex act as a cortical feedback loop, where signals from the neo-cortex are relayed through the striatum, pallidum, and thalamus back to the cortex. The cortex excites the striatum, which in turn inhibits the pallidum, thus inhibiting the thalamus. Before and during movement, the striatum activates and inhibits the pallidum, allowing greater excitation of the motor thalamic nuclei and cortex [27]. When lesions form in any of these regions of the brain as a result of stroke, a whole host of maladies including muscle synergies develop, ultimately leading to this chain of properly timed neuronal activation and inhibition becoming disrupted, and causing the person to experience "jerky" movements.

Optimal Control: Human movement, in its simplified form, can be thought of as a 3-dimensional series of points moving between two locations. As a result human movement as a whole can be modeled as a series of differential equations subject to controls that influence the behavior of the system. Further, it can be shown that, with regards to motor function, the brain can be thought of as a series of control algorithms with the intent of maximizing or minimizing some criterion or set of criteria. It has been shown that human upper extremity movements operate with intent of maximizing "smoothness". Quantitatively, this can be represented as minimization of jerk, the third derivative of displacement [28]. In the case of reach and retrieval, these actions can be modeled as a 1-dimensional system, where the trajectory of motion between two points with minimization of jerk is:

$$x(t) = x_i + (x_f - x_i)(10(t/d)^3 - 15(t/d)^4 + 6(t/d)^5)$$

where x_i is the initial displacement at t = 0 and x_f is the final displacement at time $t = d$.

The REACH was designed to, through actuated assistance, supply output torque necessary to minimize deviation from the above minimized jerk trajectory during excursions on the device. This provides the following benefits:

1. Greater Accuracy and Precision: As the device is equipped with controls specific to the minimum jerk function, the user is consistently experiencing the exact motions with which they have to travel in order to produce a smooth movement. They now, rather than having both the goal of identifying proper trajectory, as well executing it, solely need to devote their efforts to executing a predetermined trajectory provided by the REACH.

2. Learn by Repetition: It is well established that the greater number times a patient repeats a movement, the easier that movement will become in the future. An actuated device will afford a much greater number of repetitions in a single treatment than can be provided by a PT alone.

3.2 Requirements of Actuation and Control

As discussed, REACH operates by treating the patient's hemiparetic hand as a plant, closing the loop through added sensors and actuation, aligning the patient's movements with a virtual trajectory that is the minimum jerk function. Over time the patient will implicitly redevelop the utilization of minimum jerk

trajectory when reaching and flexing on their volition. In order to most effectively accomplish this, it is necessary to consider a variety of factors:

1. Sufficient Torque: The chosen motor of the REACH must have a stall torque such that it can drive the actuator with sufficient force to act as a human-in-loop controller.

2. Back-drivability: In order for the REACH to function as a human-in-loop system, the patient must be able to supply sufficient force against the motor. Excess friction in the system reduces the efficacy of the system, as the user, in not being able to overcome said friction, will have no opportunity to execute the trial-and-error process necessary for relearning minimum jerk movement. As such, friction in the system, must be minimized. Friction reduction can be divided into two categories:

    - Internal Friction: This is friction that may occur regardless of selected actuator, such as friction between linear bearings and linear shafts. This will be greater discussed in the next chapter.

    - Gearless Actuation: The conversion from rotational motion by the motor to linear motion often is achieved via a geared system. Gears, however, are well known to have high friction, and, therefore, would supply resistance force to users applying force to a geared linear actuator, regardless of any output by the actuator's motor. It is thus appropriate to choose a gearless actuator that will supply minimum resistive resistance force when moved by a user.

3. Imposing Motion or Force: Traditional control system for rehabilitation have been standard position- or force-controlled robotic arm trainers. These de-

vices have often shown minimal efficaciousness as they have been shown to violate two necessities of robotic rehabilitation:

- Spatial Autonomy: The patient need receive assistance only if they are not conformant with needs of the task.
- Temporal Autonomy: The patient is provided room for error by the controller in order to promote self-learned movements.

3.3 Go/No-Go Criteria

The chapter's exact specifications were conceived from go/no-go criteria in the implementation of closed loop SIC control for the REACH prototype.

1. Hardware: integration of motor, actuator, and driver.
2. Open-Loop Control: Pulse Width Modulation (PWM) actuation through Arduino without sensor feedback to run the motor and actuator.
3. Closed-Loop Control: Inclusion of sensor feedback with position control
4. SIC Control: Inclusion of sensor feedback with impedance control
5. Slot Control: Introduce slot control mechanics

3.4 Hardware and Mechanical Modifications

3.4.1 Motor and Actuator

In future reports, an in-depth motor and actuator selection is necessary. As this paper is meant to establish a proof of concept, this section will layout key considerations in deciding a motor and actuator and provide justifications for the

selected prototype motor and actuator but will not provide the necessary extensive calculations for a those needed in a clinical level prototype. Short calculations for potential next-phase motor and actuator will be provided in the Future Work chapter of this report.

1. Motor: The dynamic nature of UE rehabilitation requires that a motor be capable of both high speeds and high torque output. Furthermore, as the device is meant to be portable, these high speeds and torques must be achieved in a small space. Anklebot, a portable rehabilitation device, implemented Kollmorgen BLDC motors that were successful in providing necessary outputs in a compact space. These motors will be the primary consideration when choosing a motor for REACH. Due to the heavy cost of these motors, the prototype implemented the 3-phase Anaheim Automation BLY171D BLDC motor, a much cheaper and less powerful alternative of similar dimensions, yet with sufficient power output for proof-of-concept testing [29].

2. Actuator: As previously established, a gearless actuator is needed in order to maximize back-drivability. A standard in rehabilitation robotics is the Roh'Lix Linear Actuator, a threadless, mechanical, screw-type actuator utilizing element ball bearings [30]. As such, an available generic Roh'Lix actuator was utilized in the proof-of-concept prototype.

3.4.2 Electronic Hardware

1. Processing: In the training app, the sensory input is sent from the on-board Arduino to the Raspberry Pi via a serial line, which would then be processed by a python script. This series of data transfers is substantially slower than

necessary to provide dynamic outputs to the controlled motor. The control algorithm and motor output are, therefore, entirely stored in the Arduino itself, in order to minimize processing time.

2. Motor Controller: The DRV832x 6 to 60-V Three-Phase Smart Gate Driver by Texas Instruments was integrated. This controller offers a 1x mode, which allows a 3-phase BLDC motor to be controlled by a single PWM input, simplifying the interfacing between motor and Arduino.

3.4.3 Mechanical Changes

Motor Mount: The placement of the motor on the REACH was a result of two primary considerations: reduction of external moments on the device due to the motor's weight, and location that would place the motor at minimal risk of damage. It was found that the motor would best be placed at the shoulder of the REACH itself, minimizing potential for moments when the device is used in its elevated positions, as well as minimizing exposure, given that the shoulder is securely mounted to the table. As such, a shoulder mount redesign was made from PLA in order to accommodate the motor in figure 13.

Belt System and Rotary Shaft: The lower linear shaft of the BATRAC was replaced with a rotary shaft as shown in figure 14, mounted to the REACH with ball bearings. The rotary shaft was then connected to the motor by a small belt-and-pulley system as shown in figure 13.

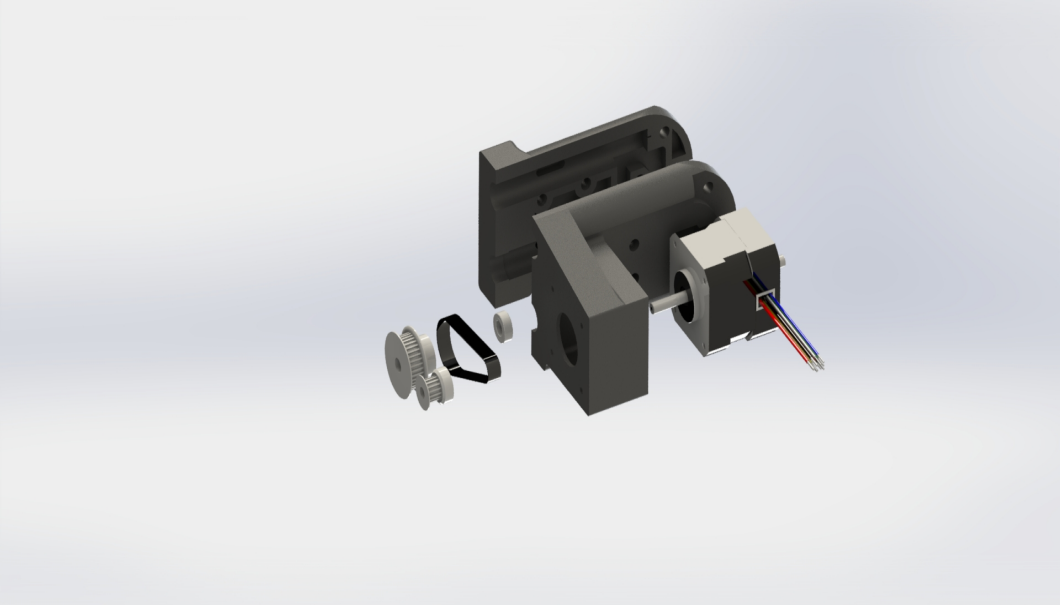

Figure 13: Exploded view of motor housing with belt and pulleys

Handle Modifications: The handle on the un-actuated BATRAC was a single component containing a linear ball bearing and a linear sleeve bearing. In order to accommodate actuation, this setup was replaced with a PLA-housed linear ball bearing on the upper un-actuated linear shaft, connected to the Roh'Lix, which in turn was connected to the added rotary shaft (bottom shaft) of the REACH. An exploded view is shown below in figure 14.

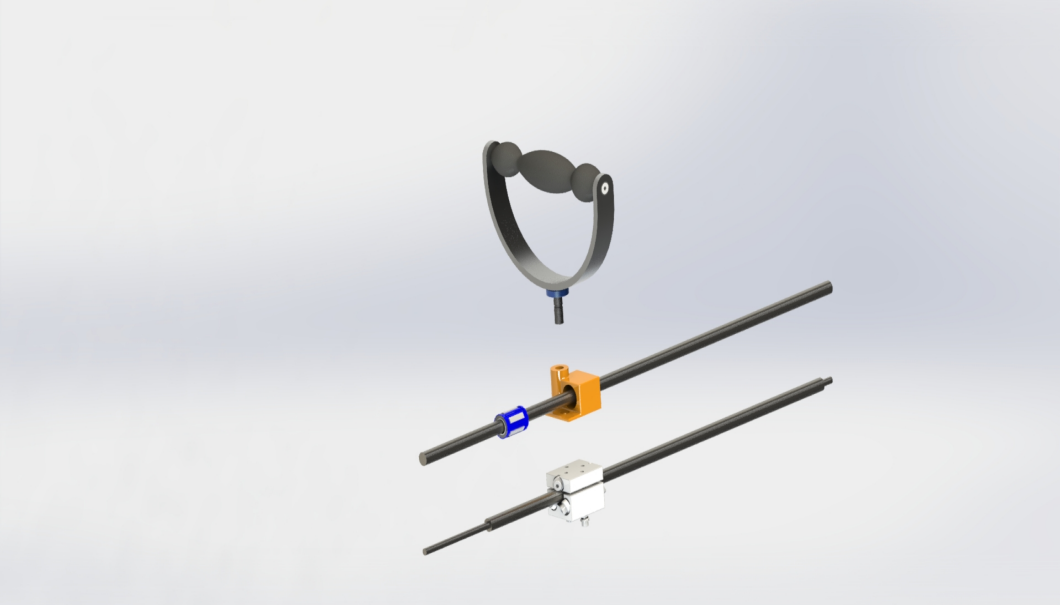

Figure 14: Exploded view of handle, handle mount, linear ball bearing, linear shaft (upper) shaft, rotary shaft (lower) and Roh'Lix

3.5 Using Input Voltage to Modulate Torque

The control laws for the REACH are principled in applying specific end-effector forces. This force is produced through a motor output torque, which is then amplified through the belt-pulley system, and transformed into linear force by the Roh'Lix actuator. In this case, the motor torque is modulated via PWM voltage output. An experiment was conducted in order to determine the associated end-effector force produced for a range of PWM outputs by the Arduino. The experimental setup is illustrated below in figure 15.

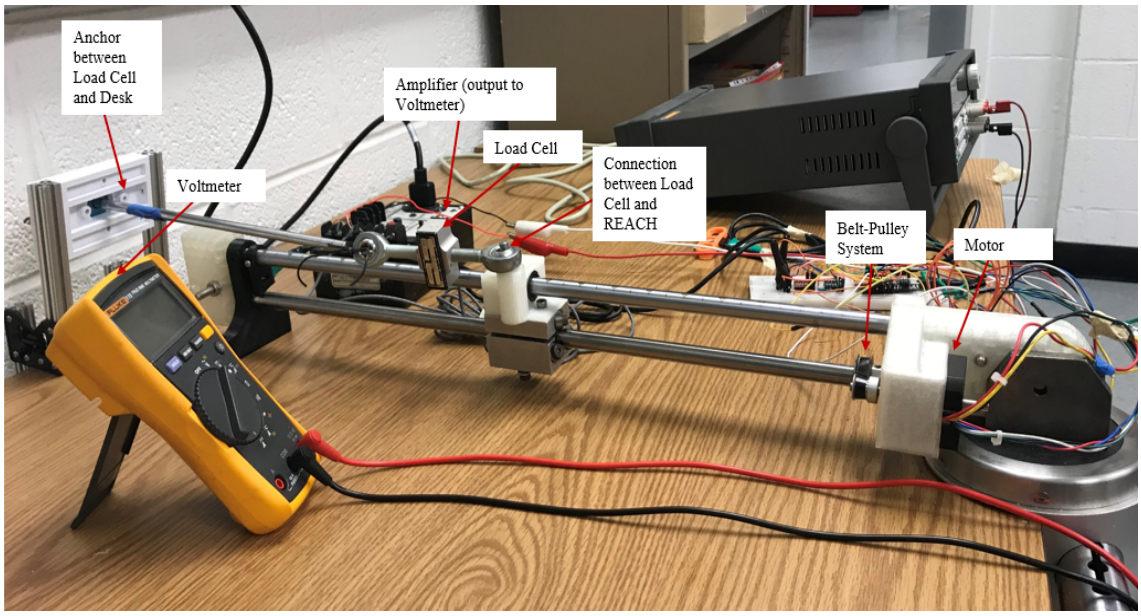

Figure 15: Load Cell on REACH

In the above experiment, a load cell was placed such that it connected a fixed space, in this case the desk, with the actuated handle mount of the REACH. A PWM signal in increments of 10% provided the motor with the equivalent percentage of the motor's maximum voltage of 24V. The force for a given PWM was delivered by supplying an initial 0 PWM and increasing the PWM signal by 3.9% duty cycle every half second in order to simulate static loading and minimize fluctuations in readings due to impulses. This caused the REACH to supply a tensile force on the load cell, which in turn was amplified by the amplifier and recorded by the voltmeter. The voltage outputs were converted into end-effector force outputs through a known conversion factor of 52.13 N/V. These values were then converted into rotary shaft torque by dividing by the specified Roh'Lix conversion factor of 33.9 N/Nm. Finally, the motor torque was then determined by multiplying by the pulleys' pitch ratio of 0.444. Three trials were

performed for any given PWM increment. The average of each set of three trials was then taken and tabulated. The results are tabulated in Appendix A. The end-effector force was then plotted against the Arduino PWM output and a line of best fit was determined. This is shown below in figure 16.

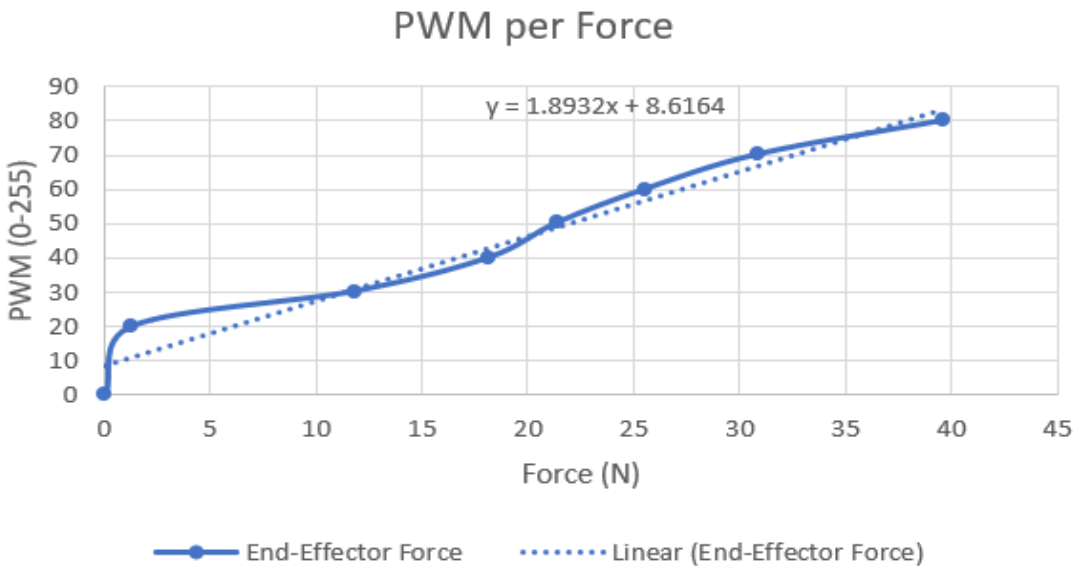

Figure 16: End-effector force for a given PWM input

From the graph above, it was determined that a linear fit was most appropriate, with a translation from desired end-effector force to output PWM of:

$$PWM = 1.8932 * F + 8.6164$$

where PWM is an Arduino output ranging from 0 to 255 bits, and F is the desired end-effector output force in Newtons. Further, by setting PWM equal to 0, it can be calculated that the static friction of the system is 4.55 N. This value is

comparable to the estimated or measured static friction in other upper-extremity rehabilitation robots such as the MIT-MANUS [31].

3.6 Control Algorithms and Software

Traditional position controllers have failed in robotic therapy because they were not designed to be passive. This led devices to either reduce user autonomy or risk contact instability. The REACH was designed on a two-fold control paradigm:

1. Simple Impedance Control: Simple Impedance Control (SIC) is a solution that renders a device passive ensuring contact stability. It does so by treating the robot controller as a spring-damper system acted upon by the virtual reference and the end-effector position via robot inertia, to provide "push" or "pull" assistance. The magnitude of "push" or "pull" are determined by the virtual spring stiffness and damping, which in practice are programmable gains of the SIC. Since the spring-damper system is always passive, the robot circumvents coupled instabilities [32]. Further, by explicitly modulating end-effector mechanical impedance rather than position or force, this minimizes the user's need to learn the robot's dynamics.

2. Slot Control: The SIC is coupled with a 1-D moving box or "slot" controller, where a virtual slot is created around each point of a virtual reference, in this case the minimum jerk trajectory. The top and bottom edges of the slot move continuously such that that they pseudo-collapse at the end of the movement. During usage, the detected position (in this case, the user's hand) is outside of the slot, the user is assisted via the SIC, where the torque output is a result of controller gains on position and velocity errors. If the user is within the bounds of the slot, a derivative control is implemented

to act as viscous cushioning. This slot control allows the user a margin of error, and therefore, permits the user both spatial and temporal autonomy.

A 1-D visual example of slot control is provided below:

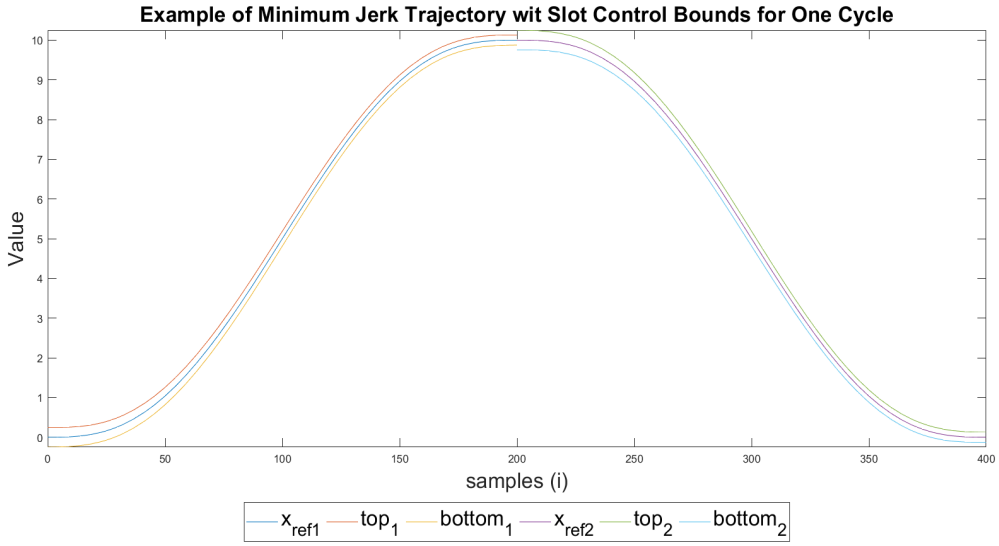

Figure 17: Slot Control Example

The above graph depicts a 2 second trajectory cycle: 1 second extension and 1 second flexion. Because sensor measurements are periodic, and therefore discrete, it is often more effective to measure time with regards to i, the number of samples taken, rather absolute time. This is reflected in the example above. As can be seen, the middle line represents the device's reference trajectory, in this case the minimum jerk trajectory across time. The lines above and below this reference are the upper and lower and bounds of the slot controller (*top* and *bottom* respectively). If the user is outside of these bounds, the controller will provide SIC assistance. If the user is inside these bounds, the controller will only provide damping assistance. Note that there is a break at the half-way point in

this cycle. A single cycle is divided into two applications: extension and flexion. In order to promote goal-oriented movement, the slot control's bounds narrow as the reference trajectory nears its final value. The bounds of the slot controller then reset at the beginning of each application. The sudden increase in bounds in the graph represents the transition between reference extension and reference flexion.

The slot control dynamics utilized by the Arduino are based on a series of well known equations. First, the reference trajectory was set as the minimum jerk trajectory, revised to be in the i^{th} sample domain rather than the time domain. In the following equations, x_{ref_1} and x_{ref_2} are the reference trajectories for extension and flexion respectively. i represents the i^{th} sample since the beginning of a full cycle. x_i is starting position, x_f is the peak reference extension, d is the total time of extension, and f is the output frequency of the kinematic sensor.

$$x_{ref_1}(i) = x_i + (x_f - x_i)\left(\frac{10i^3}{d^3f^3} - \frac{15i^4}{d^4f^4} + \frac{6i^5}{d^5f^5}\right) \tag{1}$$

$$x_{ref_2}(i) = x_f + (x_f - x_i)\left(\frac{10(f-i)^3}{d^3f^3} + \frac{15(f-i)^4}{d^4f^4} + \frac{6(f-i)^5}{d^5f^5}\right) \tag{2}$$

The bounds of the slot controller relative to the reference minimum jerk trajectory were then calculated. *top* and *bot* are the top and bottom bounds of the slot controller at any given instant and are shown below. Again, the bounds below with the subscript "1" correspond to the extension phase bounds, and those with a subscript "2" correspond to the flexion phase bounds.

$$top_1(i) = \frac{b_0}{2} + x_i + (x_f - x_i)\left(\frac{10i^3}{d^3f^3} - \frac{15i^4}{d^4f^4} + \frac{6i^5}{d^5f^5}\right) - \frac{i(b_0 - b_1)}{2df} \tag{3}$$

$$top_2(i) = \frac{b_0}{2} + x_f - (x_f - x_i)\left(\frac{10(i-fd)^3}{d^3f^3} - \frac{15(i-fd)^4}{d^4f^4} + \frac{6(i-fd)^5}{d^5f^5}\right) - \frac{(i-fd)(b_0 - b_1)}{2df} \tag{4}$$

$$bot_1(i) = x_i - \frac{b_0}{2} + (x_f - x_i)\left(\frac{10i^3}{d^3f^3} - \frac{15i^4}{d^4f^4} + \frac{6i^5}{d^5f^5}\right) + \frac{i(b_0 - b_1)}{2df} \tag{5}$$

$$bot_2(i) = x_f - \frac{b_0}{2} - (x_f - x_i)\left(\frac{(10(i-fd)^3)}{d^3f^3} - \frac{15(i-fd)^4}{d^4f^4} + \frac{6(i-fd)^5}{d^5f^5}\right) + \frac{(i-fd)(b_0 - b_1)}{2df} \tag{6}$$

F_{a1} and F_{a2} are the SIC end-effector forces modified to be in accordance with slot control dynamics and are applied when the user's position is above or below these respective bounds. F_{a3} is a damping output force applied when the user is within the bounds of the slot controller. These force outputs can be adjusted by toggling the controller proportional and derivative gains K_p and K_d. x_h and $\dot{x}_h$ are the human (or end-effector) real-time displacement and velocity respectively.

$$F_{a1} = -K_p(x_h - top_{val}) - K_d\dot{x}_h \tag{7}$$

$$F_{a2} = -K_p(x_h - bottom_{val}) - K_d\dot{x}_h \tag{8}$$

$$F_{a3} = -K_d\dot{x}_h \tag{9}$$

The function below represents the control sequence. If the cycle is in the extension phase, choose a value of 1. If in the flexion phase, choose a value of 2.

$$val = \begin{cases} 1 & \text{if } 0 \leq i < fd \\ 2 & \text{if } fd \leq i < 2fd \end{cases} \tag{10}$$

The value above is then used to select the bounds corresponding to the specific cycle phase, and thus, the necessary end-effector force to be produced by the motor given the user's spatial relationship to these bounds, as shown below.

$$F_a(x) = \begin{cases} F_{a1} & \text{if } x_h > top_{val}(i) \\ F_{a2} & \text{if } x_h < bottom_{val}(i) \\ F_{a3} & \text{if } bottom_{val}(i) < x_h < top_{val}(i) \end{cases} \tag{11}$$

The equations above, however, assume a constant sampling frequency, which is not always achievable through the current Arduino/TOF combination. As such, the Arduino itself in prototyping implemented similar *top* and *bot* equations, but in units of time rather than sampling time. These equations are shown below:

$$top_1(t) = \frac{b_0}{2} + x_i + (x_f - x_i)\left(10\left(\frac{t}{d}\right)^3 - 15\left(\frac{t}{d}\right)^4 + 6\left(\frac{t}{d}\right)^5\right) - \frac{t(b_0 - b_1)}{2d} \tag{12}$$

$$top_2(t) = \frac{b_0}{2} + x_f - (x_f - x_i)\left(10\left(\frac{d-t}{d}\right)^3 + 15\left(\frac{d-t}{d}\right)^4 + 6\left(\frac{d-t}{d}\right)^5\right) + \frac{(b_0 - b_1)(d-t)}{2d} \tag{13}$$

$$bot_1(t) = x_i - \frac{b_0}{2} + (x_f - x_i)\left(10\left(\frac{t}{d}\right)^3 - 15\left(\frac{t}{d}\right)^4 + 6\left(\frac{t}{d}\right)^5\right) + \frac{t(b_0 - b_1)}{2d} \tag{14}$$

$$bot_2(t) = x_f - \frac{b_0}{2} + (x_f - x_i)\left(10\left(\frac{d-t}{d}\right)^3 + 15\left(\frac{d-t}{d}\right)^4 + 6\left(\frac{d-t}{d}\right)^5\right) - \frac{(b_0 - b_1)(d-t)}{2d} \tag{15}$$

$$val = \begin{cases} 1 & \text{if } 0 \leq t < d \\ 2 & \text{if } d \leq t < 2d \end{cases} \tag{16}$$

3.7 Experiments and Results

In order to test the functionality of the REACH control system, the REACH was put through 5 normal-use extension excursions by the tester. Baseline gains were roughly based on those used in the MIT MANUS. The test used a K_p of 100 N/m, K_d of 2 Ns/m, and initial and final slot heights of 6 and 3 cm respectively. x_f was set to the tester's arm length of 30 cm, and x_i of 3 cm in order to minimize contact with the pulleys of the prototype, and an extension time of 10 seconds. Distance measurements and end-effector force data were collected and plotted below in figures 18 and 19.

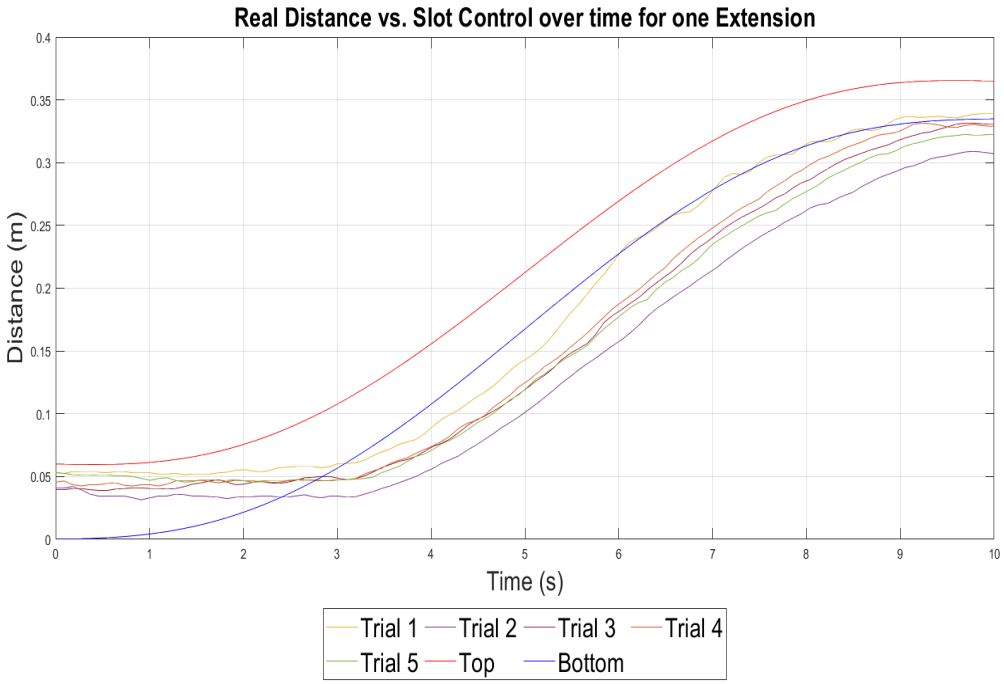

Figure 18: End-effector distance for one extension plotted over slot control bounds

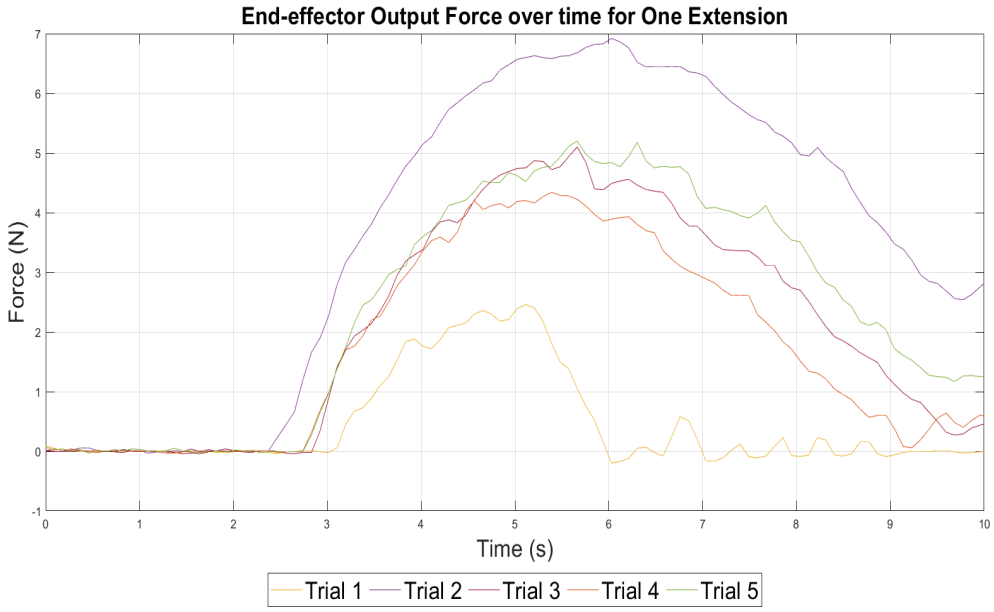

Figure 19: End-effector output force for one extension

As can be seen in figure 18, the slots themselves follow the minimum jerk trajectory as well as begin with an initial slot height of 6 cm and end with a slot height of 3 cm. Further, the trajectories themselves mimic the minimimum jerk trajectory, implying initial functionality. The performance of the device is further demonstrated by the output force in figure 19 over time. In the first 2.5 to 3 seconds of the excursion, the end-effector is inside the bounds of the slot, and the user is expected to supply minimal velocity output. This corresponds to the minimal force output shown above in figure 19. As the human trajectory begins to deviate from the bounds of the slot, the controller applies force to bring the user back to the bounds of the slot control. As the difference between real trajectory and bottom slot increases between roughly 3 and 6 seconds, the controller applied greater torque to keep the user in alignment with its corresponding trajectory. As

this difference decreases towards the end of the extension phase, the applied force in turn decreases. Trial 1 further demonstrates the successful implementation of slot control. If the user is capable of re-entering the bounds of the slot control, the control will only supply a small derivative gain force to provide a cushioning effect for the user.

4 CHAPTER 4. FUTURE WORK AND GUIDELINES

As stated, the purpose of the REACH prototype was to develop a proof-of-concept minimalist functional model, to then be expanded upon in further iterations of REACH phase 1, as well as through doing, outline key considerations when beginning development of REACH phase 1 that would not have become evident otherwise. Experiment with the BATARC as well as current REACH has succeeded in revealing necessary steps to be taken in future models of the REACH. While many of the current modifications may be permanent, development of the prototype has highlighted essential steps to be taken in future work.

4.1 App modifications

The current prototype is currently equipped with the barebones software necessary for visual feedback and kinematic data collection. In order to develop the existing software into a fully fledged clinical app, several redesigns are necessary:

Data Storage: Currently the user's clinical and kinematic information are stored locally in the REACH's on-board computer. This is very insecure, and any damage or tampering with the device could lead to patient data being lost or stolen. The data will therefore have to be stored in a way that minimizes these risks. *Suggestion*: Current considerations being explored are storing user data on a database within the company, or potentially secure online virtual storage, such as Amazon's AWS.

Accessibility to Physical Therapists: Currently the app is capable of simple data acquisition which is emailed to the PT periodically. *Suggestion*: In order for

the PT to get the best use of the app, two fundamental design changes must be implemented:

1. Clinical Regulations: The app must be fitted to comply with clinical regulations. One primary example of this is that patient data must be stored such that only the patient's healthcare practitioner knows the identity associated with the user data acquired by the REACH. One way this is often achieved is by generating an a 7-digit ID corresponding to the patient, the practitioner being the only person with access to the corresponding identity of the ID code.

2. Patient-PT Network: Currently the app is designed to accommodate a single patient and a single PT at any given time. The next step is to develop the app such that a single software, through patient and PT login information, can service any number of PTs with any number of patients. This redesign should take into specific consideration supplying the PT with an organized, flexible platform such that they can easily interact with their patients.

Inclusion of Rehabilitation Progression: *Suggestion*: Future versions of the app will come with a tab where the patient will have access to summary data on their rehabilitation progress.

4.2 Sensing and Actuation Modifications

Sensor Redesign: Although a TOF sensor, as shown, is sensitive enough for proof-of-concept prototyping, a quicker and more accurate sensor is needed. *Suggestion*: Future REACH prototypes will likely feature an optical or magnetic linear encoder for kinematic data.

Bare Metal Coding: While it is suitable for a proof-of-concept prototype, an Arduino has too slow of a processing time for rehabilitation motor controller applications. *Suggestion*: The device needs to be equipped with a controller capable of being given its native Assembly code.

Minimize Stiction: Design changes must be made in order to further minimize any non-robotic force felt by the user. *Suggestion*: Factors including material type, bearing selection, lubrication, shaft alignment, shaft design, bearing selection, and power transmission, will be further scrutinized.

Current Management: The present design modulates torque by altering voltage input. This is rather indirect, as a torque is in reality, modulated directly via the applied current, rather than the voltage. Through voltage modulation alone, although often quite accurate, does not guarantee a specific current output for a given voltage output, and as such, voltage regulation alone can only produce a motor torque within a specific confidence. *Suggestion*: Newer models of REACH will therefore feature a PID current control, which will directly modulate the applied current to the motor for more precise motor torque outputs.

4.3 Mechanical Redesigns

4.3.1 Ergonomics

Handle Ergonomics: The patient interfaces with the rehabilitation device via the handles. Usage of these handles requires constant forearm rotation or pronation, increasing strain which restricts the patient from following the natural arm movements necessary for training. The handles themselves also require the user to utilize particularly awkward finger positions. *Suggestion*: A redesign of the

handle is thus needed such that the user will be able to retain a neutral position throughout their use of the device.

Weight Reduction: The device as-is is bulky, and difficult to dis/re-assemble, making the device awkward to transport between locations. *Suggestion*: A re-design taking into consideration weight and Design for Assembly considerations is needed.

4.3.2 Structural Integrity

Elevation Backlash: The system is intended to be used in both horizontal and inclined positions to allow for training different arm motions. The current BATRAC's security allows the system to shake intensely as the patient pushes the handles along the rails of the device, thus hindering any rehabilitative effects of the device. *Suggestion*: The device must thus be redesigned to prevent any shaking of the device during operation.

Elevation Change: In order to allow the device to achieve multiple angles of elevation, the current method requires the rails of the BATRAC to be pushed into the shoulder of the device, which disengages a locking mechanism, allowing the user to change the elevation angle of the device. This method, however, invokes loose fitting attachments that contribute to the device's shakiness. *Suggestion*: A redesign is thus needed to increase stability for different elevations.

4.3.3 Manufacturability

Suggestion: After the above tasks have been implemented, scrutinized, and verified, the REACH must be redesigned for production in accordance with Design for Manufacturing (DFM) and Design for Assembly (DFA) regulations.

4.4 Conclusions

The work performed in this project has led to the first functional BATRAC device with instrumentation, control, and visual feedback, to provide enhanced therapy compared to the previous generation device. The additions listed above will be a great asset to the BATRAC. The integration and implementation of kinematic sensors opens the door to far more effective stroke rehabilitation treatment by allowing to gauge quantitatively, a patient's rehabilitation progress, as well as allowing for integration of far more sophisticated rehabilitation tools, such as an on-screen training app. The training app in turn advanced the REACH's potential efficacy as a stroke rehabilitation device by providing both visual feedback and complex goal setting. Further, the addition of an "assist-as-needed" control system is a crucial step towards developing a rehabilitation robot. This technology has already been successfully integrated in lower extremity (LE) rehabilitation robots such as Anklebot. Integration of this technology into upper extremity robotics such as REACH will likely result in a more efficacious and cost-effective rehabilitation than non-robotic physical therapy alone. Due to the key roles that patient motivation and understanding play in active physical therapy, it is expected that advanced feedback and goal setting, in combination with "assist-as-needed" control, will allow stroke patients to experience greater and more permanent rehabilitation.

5 Appendix A: PWM to Torque Table

%Duty Cycle	PWM (0-255)	V_{Out}	End-effector Force (N)	Rotary Shaft Torque (Nm)	Motor Torque (Nm)
0	0	0	0	0	0
10.196	26	0.005	0.26	0.00771	0.0034
20	51	0.025	1.30	0.038	0.017
30.196	77	0.23	11.8	0.35	0.16
40	102	0.35	18.14	0.54	0.24
50.196	128	0.41	21.37	0.63	0.28
60	153	0.49	25.54	0.75	0.33
70.196	177	0.59	30.9	0.92	0.41
80	204	0.76	39.6	1.17	0.52

Note: Current limitations only permitted the experiment to be performed up to 80% duty cycle without sacrificing voltage output.

References

[1] J. W. Stinear and W. D. Byblow, "Disinhibition in the human motor cortex is enhanced by synchronous upper limb movements." *The Journal of physiology*, vol. 543, no. Pt 1, pp. 307–16, aug 2002. [Online]. Available: http://www.ncbi.nlm.nih.gov/pubmed/12181301 http://www.pubmedcentral.nih.gov/articlerender.fcgi?artid=PMC2290478

[2] J. Desrosiers, D. Bourbonnais, L. Noreau, A. Rochette, G. Bravo, and A. Bourget, "Participation after stroke compared to normal aging," *Journal of Rehabilitation Medicine*, vol. 37, no. 6, pp. 353–357, nov 2005. [Online]. Available: http://www.ncbi.nlm.nih.gov/pubmed/16287666 https://medicaljournals.se/jrm/content/abstract/10.1080/16501970510037096

[3] M. H. Mudie and T. A. Matyas, "Responses of the Densely Hemiplegic Upper Extremity to Bilateral Training," *Neurorehabilitation and Neural Repair*, vol. 15, no. 2, pp. 129–140, mar 2001. [Online]. Available: http://www.ncbi.nlm.nih.gov/pubmed/11811254 http://journals.sagepub.com/doi/10.1177/154596830101500206

[4] A. R. Luft, S. McCombe-Waller, J. Whitall, L. W. Forrester, R. Macko, J. D. Sorkin, J. B. Schulz, A. P. Goldberg, and D. F. Hanley, "Repetitive Bilateral Arm Training and Motor Cortex Activation in Chronic Stroke," *JAMA*, vol. 292, no. 15, p. 1853, oct 2004. [Online]. Available: http://jama.jamanetwork.com/article.aspx?doi=10.1001/jama.292.15.1853

[5] A. K. Asbury, G. M. McKhann, and W. I. McDonald, *Diseases of the nervous system : clinical neurobiology.* W.B. Saunders, 1992.

[6] H. S. Jørgensen, H. Nakayama, H. O. Raaschou, J. Vive-Larsen, M. Støier, and T. S. Olsen, "Outcome and time course of recovery in stroke. Part II: Time course of recovery. The Copenhagen Stroke Study." *Archives of physical medicine and rehabilitation*, vol. 76, no. 5, pp. 406–12, may 1995. [Online]. Available: http://www.ncbi.nlm.nih.gov/pubmed/7741609

[7] C. G. Ostendorf and S. L. Wolf, "Effect of forced use of the upper extremity of a hemiplegic patient on changes in function. A single-case design."

Physical therapy, vol. 61, no. 7, pp. 1022–8, jul 1981. [Online]. Available: http://www.ncbi.nlm.nih.gov/pubmed/7243897

[8] S. L. Wolf, D. E. Lecraw, L. A. Barton, and B. B. Jann, "Forced use of hemiplegic upper extremities to reverse the effect of learned nonuse among chronic stroke and head-injured patients." *Experimental neurology*, vol. 104, no. 2, pp. 125–32, may 1989. [Online]. Available: http://www.ncbi.nlm.nih.gov/pubmed/2707361

[9] A. Kunkel, B. Kopp, G. Müller, K. Villringer, A. Villringer, E. Taub, and H. Flor, "Constraint-induced movement therapy for motor recovery in chronic stroke patients." *Archives of physical medicine and rehabilitation*, vol. 80, no. 6, pp. 624–8, jun 1999. [Online]. Available: http://www.ncbi.nlm.nih.gov/pubmed/10378486

[10] W. H. Miltner, H. Bauder, M. Sommer, C. Dettmers, and E. Taub, "Effects of constraint-induced movement therapy on patients with chronic motor deficits after stroke: a replication." *Stroke*, vol. 30, no. 3, pp. 586–92, mar 1999. [Online]. Available: http://www.ncbi.nlm.nih.gov/pubmed/10066856

[11] E. Taub, N. E. Miller, T. A. Novack, E. W. Cook, W. C. Fleming, C. S. Nepomuceno, J. S. Connell, and J. E. Crago, "Technique to improve chronic motor deficit after stroke." *Archives of physical medicine and rehabilitation*, vol. 74, no. 4, pp. 347–54, apr 1993. [Online]. Available: http://www.ncbi.nlm.nih.gov/pubmed/8466415

[12] M. Meinzer, E. Taub, T. Elbert, B. Rockstroh, and D. Bulach, "Die Fortentwicklung der Neurorehabilitation auf verhaltensneurowissenschaftlicher Grundlage," *Der Nervenarzt*, vol. 74, no. 4, pp. 334–342, apr

2003. [Online]. Available: http://www.ncbi.nlm.nih.gov/pubmed/12707702 http://link.springer.com/10.1007/s00115-003-1498-1

[13] A. C. Lo, P. D. Guarino, L. G. Richards, J. K. Haselkorn, G. F. Wittenberg, D. G. Federman, R. J. Ringer, T. H. Wagner, H. I. Krebs, B. T. Volpe, C. T. Bever, D. M. Bravata, P. W. Duncan, B. H. Corn, A. D. Maffucci, S. E. Nadeau, S. S. Conroy, J. M. Powell, G. D. Huang, and P. Peduzzi, "Robot-Assisted Therapy for Long-Term Upper-Limb Impairment after Stroke," *New England Journal of Medicine*, vol. 362, no. 19, pp. 1772–1783, may 2010. [Online]. Available: http://www.nejm.org/doi/abs/10.1056/NEJMoa0911341

[14] J. Whitall, S. McCombe Waller, K. H. Silver, and R. F. Macko, "Repetitive bilateral arm training with rhythmic auditory cueing improves motor function in chronic hemiparetic stroke." *Stroke*, vol. 31, no. 10, pp. 2390–5, oct 2000. [Online]. Available: http://www.ncbi.nlm.nih.gov/pubmed/11022069

[15] R. A. Schmidt and T. D. Lee, *Motor control and learning : a behavioral emphasis*. Human Kinetics, 2011.

[16] M. H. Thaut, G. C. McIntosh, and R. R. Rice, "Rhythmic facilitation of gait training in hemiparetic stroke rehabilitation." *Journal of the neurological sciences*, vol. 151, no. 2, pp. 207–12, oct 1997. [Online]. Available: http://www.ncbi.nlm.nih.gov/pubmed/9349677

[17] M. H. Thaut, G. C. McIntosh, S. G. Prassas, and R. R. Rice, "Effect of Rhythmic Auditory Cuing on Temporal Stride Parameters and EMG. Patterns in Hemiparetic Gait of Stroke Patients," *Neurorehabilitation and*

Neural Repair, vol. 7, no. 1, pp. 9–16, jan 1993. [Online]. Available: http://nnr.sagepub.com/cgi/doi/10.1177/136140969300700103

[18] J. A. Scott Kelso, C. A. Putnam, and D. Goodman, "On the Space-Time Structure of Human Interlimb Co-Ordination," *The Quarterly Journal of Experimental Psychology Section A*, vol. 35, no. 2, pp. 347–375, may 1983. [Online]. Available: http://journals.sagepub.com/doi/10.1080/14640748308402139

[19] J. A. Kelso, D. L. Southard, and D. Goodman, "On the coordination of two-handed movements." *Journal of experimental psychology. Human perception and performance*, vol. 5, no. 2, pp. 229–38, may 1979. [Online]. Available: http://www.ncbi.nlm.nih.gov/pubmed/528935

[20] R. C. Schmidt, C. Carello, and M. T. Turvey, "Phase transitions and critical fluctuations in the visual coordination of rhythmic movements between people." *Journal of Experimental Psychology: Human Perception and Performance*, vol. 16, no. 2, pp. 227–247, 1990. [Online]. Available: http://doi.apa.org/getdoi.cfm?doi=10.1037/0096-1523.16.2.227

[21] S. Swinnen, C. Walter, and D. Shapiro, "The coordination of limb movements with different kinematic patterns," *Brain and Cognition*, vol. 8, no. 3, pp. 326–347, dec 1988. [Online]. Available: https://www.sciencedirect.com/science/article/abs/pii/0278262688900589

[22] R. G. Carson, W. D. Byblow, and D. Goodman, "The Dynamical Substructure of Bimanual Coordination," *Interlimb Coordination*, pp. 319–337, jan 1994. [Online]. Available: https://www.sciencedirect.com/science/article/pii/B9780126792706500218

[23] J. A. Kelso and B. Tuller, "Converging evidence in support of common dynamical principles for speech and movement coordination," *American Journal of Physiology-Regulatory, Integrative and Comparative Physiology*, vol. 246, no. 6, pp. R928–R935, jun 1984. [Online]. Available: http://www.ncbi.nlm.nih.gov/pubmed/6742170 http://www.physiology.org/doi/10.1152/ajpregu.1984.246.6.R928

[24] M. H. Mudie and T. A. Matyas, "Can simultaneous bilateral movement involve the undamaged hemisphere in reconstruction of neural networks damaged by stroke?" *Disability and rehabilitation*, vol. 22, no. 1-2, pp. 23–37. [Online]. Available: http://www.ncbi.nlm.nih.gov/pubmed/10661755

[25] J. H. Cauraugh and S. Kim, "Two coupled motor recovery protocols are better than one: electromyogram-triggered neuromuscular stimulation and bilateral movements." *Stroke*, vol. 33, no. 6, pp. 1589–94, jun 2002. [Online]. Available: http://www.ncbi.nlm.nih.gov/pubmed/12052996

[26] A. Roy, H. Krebs, D. Williams, C. Bever, L. Forrester, R. Macko, and N. Hogan, "Robot-Aided Neurorehabilitation: A Novel Robot for Ankle Rehabilitation," *IEEE Transactions on Robotics*, vol. 25, no. 3, pp. 569–582, jun 2009. [Online]. Available: http://ieeexplore.ieee.org/document/4909072/

[27] A. Siniscalchi, L. Gallelli, A. Labate, G. Malferrari, C. Palleria, and G. D. Sarro, "Post-stroke Movement Disorders: Clinical Manifestations and Pharmacological Management." *Current neuropharmacology*, vol. 10, no. 3, pp. 254–62, sep 2012. [Online]. Available: http://www.ncbi.nlm.nih.gov/pubmed/23449883 http://www.pubmedcentral.nih.gov/articlerender.fcgi?artid=PMC3468879

[28] M. Yazdani, G. Gamble, G. Henderson, and R. Hecht-Nielsen, "A simple control policy for achieving minimum jerk trajectories," *Neural Networks*, vol. 27, pp. 74–80, mar 2012. [Online]. Available: https://www.sciencedirect.com/science/article/pii/S0893608011002978

[29] E. J. Rouse, L. J. Hargrove, E. J. Perreault, M. A. Peshkin, and T. A. Kuiken, "Development of a mechatronic platform and validation of methods for estimating ankle stiffness during the stance phase of walking." *Journal of biomechanical engineering*, vol. 135, no. 8, p. 81009, aug 2013. [Online]. Available: http://www.ncbi.nlm.nih.gov/pubmed/23719922 http://www.pubmedcentral.nih.gov/articlerender.fcgi?artid=PMC3705977

[30] H. I. Krebs, S. Rossi, S. Kim, P. K. Artemiadis, D. Williams, E. Castelli, and P. Cappa, "Pediatric anklebot," in *2011 IEEE International Conference on Rehabilitation Robotics*, vol. 2011. IEEE, jun 2011, pp. 1–5. [Online]. Available: http://www.ncbi.nlm.nih.gov/pubmed/22275613 http://ieeexplore.ieee.org/document/5975410/

[31] . Buerger, Stephen Paul, "Characterization and control of an interactive robot," 2001. [Online]. Available: https://dspace.mit.edu/handle/1721.1/88872

[32] N. Hogan, "Impedance Control: An Approach to Manipulation: Part I—Theory," *Journal of Dynamic Systems, Measurement, and Control*, vol. 107, no. 1, p. 1, mar 1985. [Online]. Available: http://dynamicsystems.asmedigitalcollection.asme.org/article.aspx?articleid=1403621